HHS Public Access

Author manuscript

Cell Metab. Author manuscript; available in PMC 2020 April 02.

Published in final edited form as:

Cell Metab. 2019 April 02; 29(4): 932–949.e4. doi:10.1016/j.cmet.2018.12.013.

Gene-by-sex interactions in mitochondrial functions and cardio-metabolic traits

Frode Norheim[1,2,*], **Yehudit Hasin-Brumshtein**[1,*], **Laurent Vergnes**[3], **Karthickeyan Chella Krishnan**[1], **Calvin Pan**[1], **Marcus M. Seldin**[1], **Simon T. Hui**[1], **Margarete Mehrabian**[1], **Zhiqiang Zhou**[1], **Sonul Gupta**[1], **Brian W. Parks**[4], **Axel Walch**[5], **Karen Reue**[3], **Susanna M. Hofmann**[6], **Arthur P. Arnold**[7], and **Aldons J. Lusis**[1,3,8]

[1]Department of Medicine/Division of Cardiology and Department of Human Genetics, University of California at Los Angeles, Los Angeles, CA

[2]Department of Nutrition, Institute of Basic Medical Sciences, Faculty of Medicine, University of Oslo, Norway

[3]Department of Human Genetics, University of California at Los Angeles, Los Angeles, CA

[4]Department of Nutritional Sciences, University of Wisconsin-Madison, Madison, WI

[5]Research Unit Analytical Pathology, Helmholtz Zentrum München, Neuherberg, Germany

[6]Institute of Diabetes and Regeneration Research, Helmholtz Center Munich (HMGU) and German Center for Diabetes Research (DZD), Neuherberg, Germany; Medizinische Klinik und Poliklinik IV, Klinikum der LMU, 80336 München, Germany

[7]Department of Integrative Biology and Physiology

[8]Department of Microbiology, Immunology and Molecular Genetics, University of California at Los Angeles, Los Angeles, CA

Summary

We studied sex differences in over 50 cardio-metabolic traits in a panel of 100 diverse inbred strains of mice. The results clearly showed that the effects of sex on both clinical phenotypes and gene expression depend on the genetic background. In support of this, genetic loci associated with the traits frequently showed sex specificity. For example, *Lyplal1*, a gene implicated in human obesity, was shown to underlie a sex-specific locus for diet-induced obesity. Global gene expression analyses of tissues across the panel implicated adipose tissue “beiging” and mitochondrial functions in the sex differences. Isolated mitochondria showed gene-by-sex interactions in oxidative functions, such that some strains (C57BL/6J) showed similar function

Lead contact: Aldons J. Lusis, Department of Medicine/Division of Cardiology, David Geffen School of Medicine, A2-237 Center for the Health Sciences, Los Angeles, CA 90095-1679, Phone: 310-825-1359, FAX: 310-794-7345, jlusis@mednet.ucla.edu.
*These authors contributed equally

Declarations of Interest

The authors declare no competing interests

between sexes whereas others (DBA/2J and A/J) showed increased function in females. Reduced adipose mitochondrial function in males as compared to females was associated with increased susceptibility to obesity and insulin resistance. Gonadectomy studies indicated that gonadal hormones acting in a tissue-specific manner were responsible in part for the sex differences.

eTOC blurb

Norheim and colleagues use the hybrid mouse diversity panel to comprehensively address the role of sex, and its interaction with genetic background, on cardio-metabolic phenotypes and gene expression. They discover a sex-specific obesity locus for *Lyplal1*, reveal sex-specific regulation of adipose tissue beiging and find gene-by-sex interactions for mitochondrial function.

Graphical Abstract

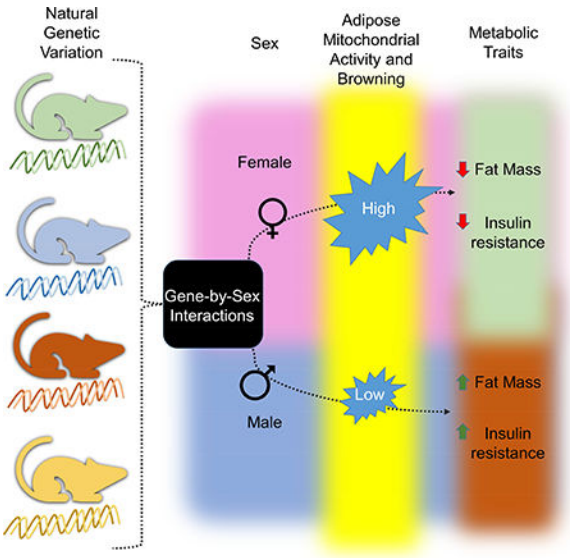

Keywords

sex differences; Hybrid Mouse Diversity Panel; gene-by-sex interactions; adipose tissue “browning”; uncoupling protein-1; mitochondrial functions; gonadectomy

Introduction

Sex differences in susceptibility to obesity, insulin resistance, and other cardiometabolic traits have been amply described in mice, humans and other species, with females generally exhibiting beneficial metabolic profiles (Karp et al., 2017; Kenney-Hunt et al., 2008; Mittelstrass et al., 2011; Ober et al., 2008; Parks et al., 2015; Varlamov et al., 2014; White and Tchoukalova, 2014; Yang et al., 2006). Sex differences have also recently been identified for the gut microbiome (Fields et al., 2017; Org et al., 2016). Gene expression studies show that a large proportion of genes are differentially expressed in adipose, liver, brain and other tissues (Della Torre et al., 2018; Kwekel et al., 2017; Yang et al., 2006), and that sex hormones as well as chromosome complement play a major role in modulation of

gene expression (Kukurba et al., 2016; Mozhui et al., 2012; Rinn and Snyder, 2005; Vieira Potter et al., 2012; Yang et al., 2006). Directly or indirectly, sex differences arise from different sex chromosome dosage, and can be either permanent or reversible in nature. Sex hormones contribute to both of these effects, but sex differences also arise independently of gonadal hormones due to sex-biased effects of X and Y chromosomes within cells (gene dosage, incomplete dosage compensation, and epigenetic effects) (Arnold, 2009; Arnold and Lusis, 2012; Bouret, 2013; Capel, 2017; Charlesworth, 1996; Chen et al., 2012; Disteche, 2012; Hager et al., 2008; Link et al., 2013; Link and Reue, 2017; McCarthy et al., 2009). For example, recent studies suggest that the sex chromosome complement plays a role in diet induced obesity (Link et al., 2013; Traglia et al., 2017).

The vast majority of previous studies examined sex differences in phenotypes, genetic susceptibility to disease or gene expression in isolation, generating trait or tissue specific results without putting them in context of genetic variation and network organization. Also only a few studies examined whether the observed differences are permanent or reversible in nature (Gregg et al., 2010; Hager et al., 2008; van Nas et al., 2009). In this work, we set out to examine the effect of sex on cardio-metabolic phenotypes in mice, with respect to phenotype-phenotype correlations, their genetic architecture and the underlying expression networks in adipose and liver. To examine gene-by-sex interactions, we performed our analyses with a panel of over 100 inbred strains of mice, known as the Hybrid Mouse Diversity Panel (HMDP). We demonstrate that not only do specific phenotypes differ between male and female mice, but the interdependencies between phenotypes, as well as the underlying genetic and molecular pathways, are distinct. Our analysis of gene expression in adipose and liver shows that sex effects are highly tissue specific. While effect sizes on gene expression are modest, they affect thousands of genes in each tissue and are physiologically relevant, as exemplified by our *Lyplal1* knockout model. To understand the nature of the tissue-specific effect of sex, we examined liver and adipose expression in gonadectomized mice and observed that, while the sex effects on gene expression in liver are largely reversible, those in adipose are not. Global expression data across the HMDP suggested that mitochondrial functions in adipose are a major contributing factor to the sex differences in metabolic phenotypes. To examine the underlying mechanisms, we isolated mitochondria from a subset of the HMDP strains and observed striking gene-by-sex interactions affecting respiration and electron transport chain complexes. Sex differences in metabolic traits were highly tissue-specific. For example, we showed that while gonadal hormones have broad effects on gene expression in liver, their effects in adipose are much more modest. Our results indicate that gene-by-sex interactions are prevalent in cardio-metabolic traits in mice and that the differences are due in part to effects on mitochondrial functions.

Results

Study design

Sex differences in experimental organisms, including the mouse, have generally been studied on a single genetic background, or in a cross between two strains. Our goal was to study sex differences in the context of genetic variation, so that we could examine interactions

between genetic background and sex. Therefore we selected the HMDP, a cohort of >100 inbred and recombinant inbred mouse strains that allows high resolution genetic mapping (Bennett et al., 2010). The renewable nature of HMDP facilitates prospective collection of data on genetically identical individuals, thus making the comparisons between different conditions or over time feasible. The HMDP mice have been studied under a variety of dietary or other environmental conditions and significant sex differences were observed in all of these studies (Lusis et al., 2016). The present studies are focused primarily on HMDP fed a high-fat, high sucrose (HF/HS) diet (hfHMDP) that was previously described in detail by Parks et al. (Parks et al., 2013; Parks et al., 2015). The diet was chosen for its similarity to a typical Western diet and relevance to metabolic disorders in human populations. Briefly, it includes 3–15 mice per sex from each of the 100 strains that were fed high-fat high-sucrose diet for 8 weeks, between 8 and 16 weeks of age. Throughout the diet, as well as, at the end of the diet, multiple phenotypes were measured (Table S1). It was not feasible in such a large study to collect data on female mice at a particular part of the estrous cycle, and we note that the reproductive phase can have a significant impact on metabolic traits, thereby contributing to nongenetic variation in female mice (Byers et al., 2012). We used expression microarrays to profile gene expression in the liver and gonadal adipose tissue of the individual mice. From a total of over 150 phenotypes examined in the hfHMDP study, we selected 59 that represented clinically significant traits such as insulin resistance, obesity, plasma lipids, and fatty liver disease (Table S1). Finally, we have tested hypotheses generated by our analyses using engineered models, functional studies of isolated mitochondria, or gonadectomy experiments on a more limited set of genetic backgrounds.

Sex differences affect interdependencies of phenotypes, gene expression and phenotype-transcript correlations

Correlation between two phenotypic measurements implies either common underlying factors or a direct dependency between the phenotypes. In addition, when one phenotype is easily measurable while the other is not, closely correlated phenotypes are often used as proxy for one another. An important question is not only whether the phenotype itself shows sex differences, but what parts of the phenotypic networks are sex-specific. Thus, we explored whether sex affects the correlation structure between phenotypes, and whether the underlying associated molecular pathways are similar between sexes. To this end we examined sex-specific phenotype-phenotype correlations on three levels: a) inter-sex phenotype-phenotype correlations (Fig. 1A); b) co-sharing of genes where expression is significantly associated with the phenotype in liver or adipose tissues (Fig. 1B); and c) tissue-specific patterns in sex-dimorphic gene expression (Fig. 1C, D).

The examined phenotypes from hfHMDP broadly represent 4 categories - blood related phenotypes (such as blood cell counts and percentages), body mass related (such as total body mass, organ weights, lean and fat masses and growth), behavioral (food intake) and metabolic (glucose and insulin measurements, liver and plasma cholesterol). As expected, we find a profound sex difference in all mass-related phenotypes, which could mostly be attributed to differences in body size (Table S1). Once corrected for body size (using kidney weight, see Materials and Methods), these differences were no longer significant. We note that this is not a perfect way to adjust and that kidney weight could also be affected by sex

differences. With the exception of granulocyte cell counts, blood related phenotypes showed no significant sex differences, consistent with previous observations in mice and humans (Karp et al., 2017). However, all of the metabolic phenotypes as well as food intake showed a profound sex difference (Table S1). Notably, although stratified body fat (BF) increase and weight gain were similar in males and females, stratified food intake was significantly higher in the females, suggesting differences in basic energy expenditure between sexes.

We compared phenotypes in males and females using pairwise bi-weight mid-correlations (a median based measure that is less sensitive to outliers than Pearson correlations) (Fig. 1A). Since many of the phenotypes are not independent, and some are mathematical derivations of others (e.g., BF percent increase is derived from total mass and fat mass), to evaluate significance we computed 1000 permutations for each pairwise comparison (>3 million permutations in total). The permuted distributions were similar between the sexes and phenotype pairs, and suggested that correlations stronger than 0.25 correspond to p-value threshold of 0.01, while those stronger than 0.34 correspond to p-value of 1e-3. A heatmap of the pairwise correlations between all phenotypes in males and females (Fig. 1A) shows that, as expected, the strong pairwise correlations are generally replicated between sexes. Yet, we could also identify differences in the correlation structure where a set of correlations was notably different (Fig. 1A, emphasis boxes). For example, in males the lean mass before HF/HS diet, and spleen and lung weights after 8 weeks of diet, are negatively correlated to most measures of body fat and cholesterol, while in females these correlations are mostly positive (rightmost versus middle bottom emphasis box, Fig. 1A). An opposite disparity was observed for correlations between red blood cell counts or hemoglobin measures to metabolic phenotypes and food intake (upper and leftmost emphasis boxes, Fig. 1A). Fig. S1 shows detailed plots of correlations for selected phenotypes in the Fig. 1A highlighted areas.

Another way to assess similarity between molecular pathways underlying or affected by phenotypes is by shared effects on gene expression. Thus, we examined the overlap between genes whose expression is associated with each phenotype in males and females using global gene expression data from liver and gonadal adipose across the hfHMDP. We picked all genes which were associated with each of the phenotypes, in either sex or tissue, at the p<1e-6 level (a permutation-based threshold for phenotype-transcript associations in HMDP equivalent to FDR=0.01) and computed the overlap per tissue per trait (Table S1). Fig. 1B shows that the proportion of overlap varies between traits and tissues, but generally does not exceed 50%.

Notably, in both tissues there are global sex effects on gene expression; thousands of genes show significant and robust, although modest, differential expression in either sex (Kukurba et al., 2016; Rinn et al., 2004; Rinn and Snyder, 2005; Roy and Chatterjee, 1983; van Nas et al., 2009; Yang et al., 2006). To analyze differential expression in the hfHMDP microarray data we filtered out probes based on technical quality parameters (such as identity to target sequence or uniqueness, see Materials and Methods for details), and prevalence of expression (intensity >4 in >75 strains in either sex). We then tested 8673 genes in adipose and 7235 in liver for sex differences in expression. Our model (=~strain+sex) included blocking on strain identity, a conservative option for multiple testing correction and adjusted p value threshold of 0.01 (see Materials and Methods). Consistent with previous

observations we identify sex differences in expression of thousands of genes in either tissue (3948 in adipose, and 3719 in liver, Fig. 1C-D) and significant overlap between the tissues (1608 regulated in both tissues, Chi.sq=39.6, p=3e-10). While our results are generally consistent with previous studies, our estimates of differentially expressed genes are notably higher. The higher estimation in our study likely stems from both the technical differences (our analysis includes more strains and mice, resulting in higher power), and differences in the experimental setup (the sex influence on gene expression in our study may be amplified indirectly by the different response to the high fat diet). In addition, our WGCNA analysis of co-expression networks in both sexes shows module preservation of the very large co-expression modules that reflect basic cellular function, but not the smaller ones representing specific biologic processes (**data not shown**).

We further explored what potentially functional aspects of adipose and liver biology are reflected by the genes that are differentially expressed between the sexes (Tables S3 and S4), and the role of sex hormones in regulating these differences. Enrichment analysis (Table S3) clearly shows an upregulation of genes involved in mitochondrial function in the adipose tissue of females relative to males. Terms and pathways that were highly enriched included “mitochondrion” (p<1e-25), “mitochondria inner membrane” (p<1e-11), “oxidative phosphorylation” (p<1e-14), electron transport (p<1e-12), respiratory chain (p<1e-11), and mitochondrial matrix (p<1e-7); all were highly significant after Benjamini-Hochberg correction. Practically all genes in the mitochondrial oxidative phosphorylation pathways showed significantly higher expression in female adipose tissues (**data not shown**).

Sex differences have strong effects on cardiovascular and metabolic traits and are affected by genetic background

Previous studies with the HMDP examined phenotypes in male and female mice under a variety of diets and other environmental conditions. These studies showed profound sex differences in metabolic phenotypes related to obesity (both on chow and high fat diets), insulin resistance, fatty liver, plasma lipids, atherosclerosis, and gut microbiota (Lusis et al., 2016). In some cases, such as insulin resistance (Fig. 2A) and atherosclerosis, one sex is much more susceptible than the other, whereas in other cases the differences are more modest. Yet, in all cases the genetic background appears to perturb the sex differences, and sometimes even reverse them, exemplifying abundant gene-by-sex interaction (G×S) in the metabolic phenotypes. Fig. 2A and Table S2 show examples of six phenotypes in hfHMDP (HOMA-IR, HDL, plasma TG, fat mass, body fat % growth and body fat % after 2 weeks of diet) that show sex differences across strains, but also exemplify the substantial effect of genetic background on the sex differences.

Sex specific loci in genome-wide association studies

To examine the extent to which mapping of traits overlaps between males and females we remapped all QTL loci identified by Genome-Wide Association Studies (GWAS) in males and females separately. Mapping was performed with Fast-LMM with correction for population structure using a False Discovery Rate of about 1% as previously described (Bennett et al., 2010; Lusis et al., 2016; Parks et al., 2013; Parks et al., 2015). Among the 59 traits, we were able to map significant loci for 49. Many of these loci exhibited significant

association in one sex only. In typical GWAS carried out in humans or linkage studies in outbred or F2 mouse crosses, limiting the analyses to one sex would cause a significant loss of power because it would reduce the number of recombination events encompassed by each cohort. However, in the HMDP both male and female cohorts represent the same strains and, thus, the same compendium of genotypes and recombination events. Therefore, in this setting, sex segregation only affects the mapping power to the extent that it affects the accuracy of average strain phenotype value. This can in turn reduce, improve or have no notable effect on the accuracy of GWAS mapping, depending on the number of mice in each group, the variance of the phenotype within each sex, and the true difference in phenotype mean between the sexes. Since sex differences in phenotypes are prevalent and significant (Table S1), it stands to reason that segregating the analysis by sex will potentially increase the power to map loci.

Overlap of GWAS loci can be assessed at various resolutions. While HMDP mapping resolution is typically ~3Mb, locus specific LD structure can produce substantial long-range effects and wide mapping peaks. Thus, it is not always clear if two peaks on the same chromosome truly represent distinct QTLs. Therefore, in this analysis we counted an overlap if a locus resides on the same chromosome in both sexes, which in our opinion represents the lowest, most conservative estimate of overlap. Surprisingly, even at this resolution we clearly see that a majority of QTLs do not overlap between sexes, even if we only consider traits that map in both sexes (Fig. 2B). Consistent with the idea of genetic effects on sex specificity of phenotypes, we observe clustering of sex specific loci for multiple traits. For example, loci on chromosome 17 contribute to multiple fat mass related phenotypes in males (Fig. 2B), and QTL on chromosome 15 contributes to HOMA-IR and cholesterol levels only in females, while the same traits were mapped to chromosome 9 in males. In contrast, 7 out of 10 common traits mapped to chromosome 7 in both sexes (Fig. 2B). Importantly, lack of overlap between loci can also be affected by threshold effect - i.e. a locus may just pass the significance threshold in one sex, and approach it in another. Undoubtedly, some of the identified sex-specific loci reflect differences in effect size between males and females. However, some of the loci show a strong association in one sex and no evidence of association in the other (see for examples in Fig. 2B, Fig. 3 and Fig. 4).

Sex specific estimates of broad sense heritability (H^2, Fig. 2B) also suggest that there is substantial sex specificity in genetic contribution to the observed variance in our phenotypes. It is noteworthy that for many of the traits measured, heritability was lower in females than males. It is likely that this is explained in part by the reproductive phase of females. As discussed above, it was not feasible to control for the reproductive cycling of females in our study. This additional noise in females would also impact the strength of association in GWAS studies.

Systems genetics approach elucidates sex-specific loci of clinical traits

Given that we observed striking sex-specific differences in phenotypic traits and consequent heritability measures, we next searched for genetic loci which significantly associate to clinical traits exclusive to one sex. Therefore, genome-wide significant ($p < 4.1e-6$) SNPs which map to relevant traits (above) were obtained for one sex and filtered for the entire

chromosome being below this threshold in the other (some examples are highlighted in Fig. 3). These would reflect loci for indicated clinical traits, whereby the candicate regions are exclusively observed in only one sex. Initially, we filtered the Peak SNPs for these loci for those which are also cis-eQTLs for adipose tissue genes. Upon examination of the cis-eQTLs and correlations in both sexes, we felt it best to make less assertive conclusions behind which specific genes could underlie this sex-specific response. One consideration in using cis-eQTL to prioritize candidate genes is that in general, only a small fraction of total variation in gene expression is explained in cis. Given that there are a substantial number of genes within these regions which are also cis-eQTLs for expression in adipose tissue (or liver) and that, in general, cis-regulation of gene expression explains a very small fraction of the variance, all proximal genes are shown in Fig 3. Here we provide several potential candidates which could play important roles depending on the tissue and sex. Collectively, we are able to demonstrate several notable gene-by-sex interactions through identification of genetic loci which are likely driving variations in cardiometabolic traits predominantly in one sex.

Validation of a gene polymorphism affecting response to a high fat diet in females but not males: *Lyplal1*

The BF% in the hfHMDP was measured bi-weekly over 8 weeks of diet. Association mapping of BF% after 2 weeks of a HF/HS revealed a female specific locus on Chr1 (Fig. 4A). This locus encompassed only one gene, *Lyplal1*, which is also a GWAS candidate in human obesity studies (Heid et al., 2010; Lindgren et al., 2009). *Lyplal1* has a deleterious missense mutation rs31134248 (I58T, as predicted by the PROVEAN prediction algorithm, Fig. 4B) (Choi and Chan, 2015), which is also the strongest *local* (and presumably *cis*-acting) expression quantitative trait locus (*local*-eQTL) in adipose tissue of males (p = 3e-20), while in females the strongest *local*-eQTL is rs32885362 (p = 1.44e-25, Fig. 4C). Both of these SNPs reside close to each other and are in high linkage disequilibrium.

To investigate potential mechanisms underlying the sex difference, we compared *Lyplal1* expression between the sexes. Females showed significantly higher adipose *Lyplal1* expression levels than males (P = 6.47e-47, Fig. 4D). Furthermore, females, but not males, showed a significant negative correlation between adipose *Lyplal1* expression and BF% after 2 weeks of HF/HS feeding (Fig. 4E). Moreover, the SNP coding for the detrimental missense mutation (rs31134248) showed a significant association with BF% after 2 weeks of HF/HS diet in females (p = 2e-4) but not males (p = 0.53). Pathway enrichment analysis of the genes correlating most strongly with *Lyplal1* expression in female adipose tissue revealed significant enrichment for genes involved in oxidation and mitochondria (Fig. S2A). Similar pathway enrichment for *Lyplal1* was observed in male adipose tissue (data not shown).

To test whether variation in *Lyplal1* underlies the BF phenotype, we studied whole body knockout (KO) mice for *Lyplal1* in strain C57BL/6N mice (C57BL/6J and C57BL/6N are closely related substrains). In order to replicate the conditions of the to hfHMDP, the *Lyplal1* KO, heterozygous (Het) and wild type (WT) mice were fed a HF/HS diet for 2 weeks and their BF% was monitored before and after the study. Consistent with the dietary and sex

specificity of the GWAS loci, we observed no difference in BF% among the three genotypes at baseline (0 week of HF/HS) when fed a chow diet. After 2 weeks of HF/HS diet, the female KO mice showed a significant higher BF% than both the WT and Het mice taken together (Fig. 4F). This was not observed in male mice (Fig. 4F). A similar female-specific difference in the KO mice (compared to Het and WT mice) was observed for BF% growth at the same time-point (Fig. 4G). These observations indicate that *Lyplal1* has a protective effect uniquely in femalesagainst the fat mass gain in response to switching to a HF/HS diet. We note that strain C57BL/6J mice are not unusual in the level of expression of *Lyplal1* in adipose, with levels that are average (males) or slightly below average (females) as compared to the other HMDP strains (Fig. S2B).

Gonadectomy studies indicate that gonadal hormones largely account for sex differences in adult liver but not adipose

One molecular model of hormonal regulation of gene expression is based on binding of sex-biased transcription factors to DNA, similarly to other regulating cascades. Sex specificity in this model arises from circulating levels of gonadal hormones, and consequently may be thought of in general terms - i.e. if a gene is regulated, for example, by estrogens in one tissue it is likely to be regulated by estrogens in other tissues, as long as the tissues express one of the estrogen receptors. Few explicit examples of tissue specific regulation of particular genes by gonadal hormones (or tissue-by-sex interactions) have been described, but to the best of our knowledge, no studies so far examined the overlap between tissues.

In this work, we compared the extent of sex regulation of gene expression between adipose and liver on both chow and HF/HS diets using gonadectomy (GDX) experiments. Both datasets clearly indicate prevalent tissue-by-sex interactions on regulation of gene expression. In intact mice the first two principal component analysis (PCA) axes correspond, as expected, to sex and diet (Fig. 5). However, PCA of intact and gonadectomized mice generated strikingly different trajectories of shift in gene expression in adipose and liver. Specifically, in liver gonadectomy of males resulted in a shift in gene expression profile towards that of intact or gonadectomized females (PC1 in Fig. 5B, Fig. S3A), while in adipose the gonadectomized samples were not closer to the other sex (Fig. 5A). These observations are consistent with previous studies of gonadectomized male mice with regard to liver transcriptional regulation (Jalouli et al., 2003), some of which could be reversed with hormone replacement (Falls et al., 1997; Tai et al., 2003). Second, with the exception of chromosome Y and several chromosome X genes, in both datasets there was no evident correlation between sex effects on gene expression in the adipose and liver (Fig. 5C). To test whether the large shift in gene expression following gonadectomy in males was due to loss of testosterone, we carried out hormone replacement. Indeed, following testosterone (DHT) treatment, the expression of selected genes which contributed substantially to the variation in PC1 (Fig. S6) affected by gonadectomy shifted back to intact levels (Fig. 5E). These show that genes which are driving the shifts in transcriptome following gonadectomy can be reversed following hormone replacement.

To examine the possibility that differences in gene expression between sexes or following gonadectomy were due to changes in cell composition, we performed deconvolution

analyses. We used an existing deconvolution method (SaVanT, http://newpathways.mcdb.ucla.edu/savant) to assess cell type composition of the adipose samples from the hfHMDP survey and the gonadectomy experiments. Based on gene expression, the primary component in all adipose samples consisted of adipocytes across all groups (Fig. 5F-H), and there were no apparent differences in cell type composition between the sexes or as a result of gonadectomy (Student's t-test p-value = 0.991).

Gene-by-sex-by-tissue interactions affecting gene expression

Next, we explored whether regulation of gene expression as a function of genetic background is shared between sexes. Genetic regulation of gene expression may manifest in a tissue- or sex-specific manner if, for example, the genetic variant affects a regulatory element active only in one tissue or sex. Tissue specific regulation of gene expression is well documented in mouse and human eQTL studies, but the extent of gene-by-sex interactions is not well understood. To look at gene-by-sex and gene-by-tissue interactions, we compared the overlap in *local* eQTLs in both a tissue- and sex-specific manner (Fig. 5D). Specifically, we generated four separate *local*-eQTL lists (within 5Mb of the gene) for each tissue and sex, and compared the overlaps of genes with *local*-eQTLs between those lists. To avoid biasing our counts by genes that are only expressed in one tissue, this analysis was limited to genes expressed in both adipose and liver tissues in at least one sex (i.e. the overlap of lists used for analysis of sex differences in the two tissues). We labeled the genes as "Common"- those that have a *local*-eQTL in 3 or all 4 datasets, "Liver" or "Adipose"- those that have a *local*-eQTL only in liver or in adipose, "Sex-specific" - detected in only one sex but in both tissues, and "Reciprocal" - detected in one sex in one tissue, but in another sex in the other tissue. We regard the proportion of "Reciprocal" set as an approximation of overlap that is independent of either sex or tissue. Notably, among all the genes that have *local*-eQTLs, 26–32% were shared by both tissues, while 58–64% were specific to either tissue. Within each tissue only ~50% of eQTLs are shared between sexes, and 50% are sex-specific - suggesting that gene-by-sex interactions are prevalent within a tissue context. In contrast to the abundance of sex-specific regulation in a tissue specific context, the 'sex-specific' and 'reciprocal' groups were only 1–2% of the genes, suggesting that cross-tissue gene-by-sex regulation of gene expression is very limited.

This analysis may be biased in 2 ways: first, eQTLs may be just above the threshold in one sex and below (for example, due to increased noise) it in the other. In such cases, one expects to see better overlap as the threshold becomes more and more stringent. The proportions of all groups remained stable across different p-value thresholds for *local*-eQTLs (Fig. 5D), suggesting that the results are not significantly affected by lower confidence data. Second, local eQTL lists could be biased by sex differences or tissue differences in total expression, in which case we would be more likely to detect sex-specific eQTLs in the higher expressing sex or tissue. However we did not observe inter-group differences in the average expression of the *local*-eQTL genes, or in sex specificity of their expression (Fig. S4).

Global sex differences in gene expression highlight mitochondrial function in the adipose

Interestingly, and consistent with the enrichment analysis, one of the most significantly differentially expressed genes in adipose tissue was *Ucp1* (~25 fold F>M, p<1e-17, Fig. 6A). *Ucp1* encodes uncoupling protein 1, a protein carrier in the inner mitochondrial membrane with an important physiological role in thermogenesis through the dissipation of oxidation energy as heat. UCP1 activity is high in brown adipose tissue, and may be induced under some conditions in white adipocytes (often known as adipose tissue “beiging”). Both of these are generally associated with an improved metabolic profile (Cannon and Nedergaard, 2004; Giordano et al., 2016). *Ucp1* expression in adipose tissue was significantly correlated with adipose related traits in both males and females. Surprisingly, the correlations were in the opposite direction in the 2 sexes (Fig. 6B, C and Fig. S5). Specifically in females, increased *Ucp1* expression was correlated with better metabolic profiles while in males the expression of *Ucp1* seemed to reflect poorer response to high fat diet, increased insulin resistance and larger fat mass accumulation (Fig. 6B, C). Moreover, while in females *Ucp1* expression was significantly correlated with other key genes in the browning process, such as the transcription factor *Ppargc1a*, these correlations were not observed in males (Fig. S6). *Ucp1* did not exhibit a significant local eQTL and, therefore, the genetic variation in transcript levels is regulated *in trans*.

Based on the above evidence we have examined adipose tissue morphology, evidence for browning and the extent to which these differences are regulated by sex-hormones and diet in sham operated and gonadectomized C57BL/6J mice (Fig. 6D-L). First, we extended our initial findings that *Ucp1* is more highly expressed in female gonadal fat (Fig. 6A and Fig. S6) to the protein level (Fig. 6D). Our results suggest that both HF/HS diet and sex-hormones regulate *Ucp1* levels in the females (Fig. 6D), while almost no *Ucp1* staining was detected in the males (with the exception of one sample in the gonadectomized chow group, Fig. 6G). The effect of gonadectomy on *Ucp1* in females was confirmed using mRNA levels, although the fold-change was much smaller than that observed using protein staining of adipose (Fig. S3B).

Next, we investigated if the ratio of large to small adipocytes was affected by gonadectomy in C57BL/6J, C3H/HeJ and DBA/2J mice fed either a chow or a HF/HS diet. Whereas no effects of gonadectomy were observed in male mice fed either diet, gonadectomy increased the number of large adipocytes in female mice fed a chow diet (Fig. 6M). The effect of gonadectomy on adipocytes reached significance in C3H/HeJ and DBA/2J. No effect of gonadectomy on was observed on the ratio of large to small adipocytes in female mice fed a HF/HS diet. These data suggest that a sex hormone-by-diet effect exists in females and that the protective effect of female sex hormones on adipocyte size is ablated by an unhealthy diet.

Gene-by-sex interactions affecting isolated mitochondria

We evaluated mitochondrial number and function in male and female mice from three different inbred strains fed a chow diet - A/J, C57BL/6J and C3H/HeJ (Fig. 7). First, we measured the amount of mitochondrial DNA (Fig. 7A). In A/J and C3H/HeJ, but not C57BL/6J mice, females showed higher content of mitochondrial DNA than males. Next, we

investigated whether we could find a sex difference in mitochondrial respiration after normalization to mitochondrial content. We isolated mitochondria from white adipose tissues (gonadal and inguinal) and measured respiration of specific mitochondrial respiratory chain complexes. In A/J and C3H/HeJ mice, respiration from gonadal adipose mitochondria was higher in female than male mice in all complexes (Fig. 7B, C), with respiratory chain complexes II and V as well as maximal respiration rates showing around a 2-fold difference. The increase in respiration in females was due to both coupled and uncoupled respiration. In contrast, no significant differences were observed in the commonly used strain, C57BL/6J (Fig. 7D). Similar results were obtained with inguinal mitochondria (data not shown). To examine if this sex difference was dependent on diet, we repeated the study on gonadal adipose tissue from A/J and C57BL/6J mice after 8 weeks of HF/HS feeding (Fig. S7). Similar to our chow fed mice, we found increased mitochondrial respiration in females as compared to males in A/J mice (Fig. S7A). In contrast, we observed a significant increase only in the uncoupled respiration in C57BL/6J females as compared to their male counterparts when fed a HF/HS diet (Fig. S7B). Though *Ucp1* expression is higher in C57BL/6J females under both dietary conditions, we believe that external stimuli such as excess caloric intake during HF/HS treatment or additional modifiers may be needed to functionally activate UCP1-mediated uncoupled respiration in C57BL/6J females. However, this was not required for A/J and C3H/HeJ. Consistent with changes in mitochondrial respiration, female A/J and C3H/HeJ mice showed enhanced protein content of several mitochondrial electron transport chain complexes as compared to males (Fig. 7E-G). C57BL/6J mice also showed a tendency for increased protein content of several mitochondrial electron transport chain complexes in females as compared to males, but these differences did not reach significance (Fig. 7H). These results demonstrate a gene-by-sex interaction affecting mitochondrial function in mice. Notably, when challenged with a HF/HS diet, A/J was the most resistant to weight gain, C57BL/6J the most susceptible, and C3H/HeJ intermediate (Parks et al., 2013).

Discussion

We report a comprehensive study of gene-by-sex differences in cardio-metabolic traits in a panel of about 100 genetically diverse inbred strains. Several conclusions have emerged from these studies. First, we observed prevalent gene-by-sex interactions in the cardiometabolic traits studied and in regulation of gene expression in adipose and liver. Second, we obtained significant evidence for sex-specific GWAS for cardio-metabolic traits in mice, and we validated a sex-specific gene for diet-induced obesity, *Lyplal1*. Third, we used transcriptional profiling of liver and adipose to explore the basic functions affected by sex in those tissues, and found that sex affects regulation of gene expression in tissue-specific manner with strong genetic interactions. Notably, gonadectomy studies indicated that the gene expression differences between sexes in liver but not adipose were largely due to reversible hormonal effects. The gene expression studies strongly pointed to an important role of adipose mitochondria in the sex differences. This was confirmed using immunohistochemistry of adipose and functional analyses of isolated mitochondria. Each of these points is discussed in turn below.

The cardio-metabolic traits studied here exhibit striking sex-specific interdependencies, as evidenced both by trait-trait correlations and by the specificity of trait-transcript correlations. This is consistent with results of some previous studies (Traglia et al., 2017) and suggests the existence of common sex-specific higher order interactions rather than pathways that perturb individual traits. Gene expression is an important mediator of sex-specific effects and of common genetic variation, but our understanding of how gene-by-sex interactions modulate gene expression variability is limited at best. Our findings emphasize the high degree of tissue specificity for sex effects on expression. This manifests in almost complete independence of sex effects on gene expression in adipose and liver, and in tissue specificity of gene-by-sex eQTLs. Notably, we find that ~80% of eQTLS which are shared between tissues are also shared between sexes, while only ~50% of tissue specific eQTLs are shared between males and females. Concurrently, we also show that hormones have tissue-specific effects on transcriptome measures. Together, these results suggest profound differences between male and female tissues at the very basic, cellular function as well as tissue composition.

Very few studies addressing gene-by-sex interactions at the level of cardio-metabolic phenotypes have been reported (Andreux et al., 2012; Dimas et al., 2012; Liu et al., 2012a; Myers et al., 2014; Rawlik et al., 2016). In general, sex differences in the genetic architecture of human disease (Afshari et al., 2017; Chen et al., 2017; Kwon et al., 2017; Lu et al., 2017) and anthropometric traits (Karp et al., 2017; Kukurba et al., 2016; Nookaew et al., 2013; Palmer and Clegg, 2014; Randall et al., 2013b; Weiss et al., 2006; White and Tchoukalova, 2014) are suggested by some studies, yet others failed to find evidence for prevalent sex specific genetic associations in the mouse and human (Krohn et al., 2014). Our results clearly indicate that gene-by-sex interactions are common in mice, at least for metabolic traits. The importance of gene-by-sex interactions is further supported by the finding that GWAS loci in mice frequently exhibit sex-specific effects. This finding contrasts with GWAS results in human studies, where few instances of sex-specific loci have been reported (www.ebi.ac.uk/gwas/) (Liu et al., 2012b; Randall et al., 2013b). The explanation for this discrepancy is unclear and likely arises from more than one reason. It may be that sex differences are more pronounced and prevalent in mice, in which case mapping of traits in sex specific manner increases the power to map loci in mice. Another possibility is that among the mouse loci there are false positives - which in turn contribute to the sex specificity. However, sex-specific QTL have also been noted for metabolic and other traits using traditional intercrosses in mice (Melo et al., 1996; Wang et al., 2006). Another likely contributing factor is that human GWAS analyses are rarely reported separately for males and females, where sex is frequently used as a factor in linear regression model rather than in separate analysis. The validity of such approach depends on the actual difference between sexes relative to sample size, but in general this inherently reduces the power to identify sex specific QTLs. As shown here for mice, gene-by-sex interactions are prevalent, and the use of regression models is likely to obscure both the effects of sex and genetics. In general, human GWAS identify modest effects and the sample sizes required to have a robust mapping are in the tens to hundreds of thousands. Dividing that sample into two separate groups will often result in unacceptable reduction in power, even if the proportion of each sex in these groups is roughly 50%.

We examined one sex-specific GWAS locus for adiposity in detail and identified *Lyplal1* as the underlying gene. *Lyplal1* deficiency in female mice significantly increased BF% growth during the first 2 weeks of the HF/HS diet, indicating that *Lyplal1* protects against fat mass gain after switching to a diet rich in refined sugar and fat. This effect was not observed in male mice suggesting that the observed gene-by-diet effect of *Lyplal1* is specific for females. It is unclear whether the missense variant or the *cis*-eQTL, or both, are driving the sex-specific effect on body fat gain in response to the HF/HS diet. The fact that the heterozygous *Lyplal1* KO mice are very similar to the WT mice suggests that the effect is not dose dependent. This would be consistent with the scenario in which a strongly damaging missense variant is responsible. A likely mechanism explaining the sex-specific locus is that the function of *Lyplal1* is more important in females than males. This is not only supported by the sex-specific GWAS mapping, but also by the fact that *Lyplal1* is more highly expressed in female mice. The magnitude of the change we observed in the KO experiment was approximately half of the allelic effect seen in the hfHMDP. A likely explanation for this is that there are interactions between the differing genetic backgrounds of the inbred mice and the genetic variation at the rs31134248 locus. It is also possible that we would observe a larger effect of knocking-out *Lyplal1* in one of the female strains with higher *Lyplal1* expression since female strain C57BL/6J mice exhibit relatively low *Lyplal1* expression compared to most hfHMDP mice. Several human GWAS studies have identified SNPs close to *Lyplal1* that associate with waist-to-hip ratio in women but not men (Heid et al., 2010; Lindgren et al., 2009; Randall et al., 2013a). In addition, Fox and colleagues showed that a SNP close to *Lyplal1* is associated with visceral to subcutaneous adipose tissue ratio in women (Fox et al., 2012). A recent study found no significant effect of *Lyplal1* deficiency on adiposity in mice (Watson et al., 2017). However, in accordance with our data they found a tendency for increased adiposity in the female, but not in male, *Lyplal1* KO mice. The discrepancy between the data might be explained by the number of mice included (our study included more mice) in the study or a difference in diets used.

We examined the basis of the sex-dependent differences in gene expression. Tissue specificity of eQTLs is well documented, and results from a GTEx consortium that compared eQTLs identified in >40 human tissues suggests that up to 20–50% of local eQTLs are tissue specific). However, very few studies have addressed the sex specificity of eQTLs. A recent study in human blood monocytes focused on ChrX variants only (Castagne et al., 2011), while mouse eQTL studies either examined this question in a limited subset of genes or in intercrosses of only 2 strains (Yang et al., 2006). Our data suggests that while thousands of genes are differentially regulated between males and females in each tissue, only a small proportion of these differences are due to local gene-by-sex interactions. This is similar to results from some human studies (Dimas et al., 2012; Trabzuni et al., 2013; Yao et al., 2014). Therefore, it appears that the sex-specific differences in gene expression that are influenced by genetic background are regulated largely in *trans*. This is consistent with our findings discussed above that the basis of sex differences involve higher-order interactions, such as alterations of mitochondrial functions. Our data also shows that gonadal hormones play a major role in modulating gene expression in metabolic tissues, but their effects in each tissue are distinct. Genes encoded by the X and Y chromosome showed common patterns of sex-specific regulation in the two tissues, probably because of shared patterns of

sex bias caused by escape from X inactivation (leading to higher expression in XX than XY cells), and male-specific expression of Y genes involved in basic cellular functions (Arnold, 2017; Bellott et al., 2014). Otherwise, however, the pattern of sex-specific regulation in the two tissues was almost entirely different. When we used total transcriptome for PCA of gene expression (Fig. 5) it was evident that sex and diet represent the first 2 PCs in intact mice, accounting for >70% of the variability in gene expression. PCA with gonadectomized mice showed that in liver the removal of male gonadal hormones resulted in a dramatic shift of male expression such that they resembled those in females, while gonadectomy had only a modest effect on gene expression in females. Notably, in liver the effect was almost completely aligned with the sex principle component (PC1), suggesting that diet (represented by PC2) and gonadal hormones generally exert independent effects on liver gene expression. Strikingly, in the adipose, the pattern of gene expression was only modestly affected by gonadectomy in both males and females, and the direction of the shift was not along the male-female axis. These results suggest that male gonadal hormones (presumably testosterone) are critical for continuous sex-specific regulation in liver and that the sex differences in adipose might result more from organizational hormonal effect (developmental and permanent) or sex chromosome effects (Arnold, 2017).

We have followed up the global expression differences by examining adipose metabolism in more detail. We observed significant differences in the size of adipocytes, with females generally exhibiting smaller adipocytes on both chow and high fat diets. This difference was partly eliminated by gonadectomy, supporting a role of gonadal hormones. The gene expression analyses supported a role of mitochondria in the sex differences and, in particular, we observed that *Ucp1* was expressed more highly in female adipose. We confirmed this difference using immunohistochemical staining. To determine whether there were functional differences, we isolated mitochondria from three strains with highly divergent sex differences, C57BL/6J, C3H/HeJ, and A/J. We observed particularly striking differences in mitochondrial functions in C3H/HeJ and A/J, where the oxygen consumption in females was approximately twice that in males (Fig. 7B, C). Notably, the difference was much reduced or absent in the commonly used strain C57BL/6J, providing a striking example of a gene-by-sex interaction at the molecular level (Fig. 7D). Corresponding differences in the electron transport chain components were also observed in A/J, C3H/HeJ and C57BL/6J mice (Fig. 7E-H). Many studies, primarily of strain C57BL/6J, have observed that females are more resistant to diet-induced obesity and measures of insulin resistance (Karp et al., 2017; Lovejoy et al., 2009; Parks et al., 2015; Varlamov et al., 2014; Yang et al., 2006), but the mechanisms involved have been unclear. In studies across the HMDP strains, we have observed that this is not a strain-specific finding for insulin resistance, although for certain strains, females are more susceptible to diet-induced obesity (Fig. 2). In our analyses of strain C57BL/6J mice fed a high fat diet, we observed higher uncoupled respiration in females compared to males, which may partly explain this resistance (Fig. S7). Previously it has been reported that high fat diet feeding increased gonadal fat depot weight by adipocyte hypertrophy and hyperplasia in females but hypertrophy alone in male mice (Wu et al., 2017). Furthermore, estrogens protected female mice that underwent ovariectomy from adipocyte hypertrophy and from developing adipose tissue oxidative stress and inflammation (Stubbins et al., 2012). Our findings are in line with reports of a metabolically more active

gonadal white adipose tissue of female mice compared to male mice that was characterized by enhanced lipolysis and recruitment of brown adipocytes (Dobner et al., 2017; Kim et al., 2016). Moreover, there is growing evidence for a role of mitochondria in pathologies with sex differences (Silkaitis and Lemos, 2014; Ventura-Clapier et al., 2017). Given that the expression of *Ucp1* and other markers of gene mitochondrial function are strongly correlated with metabolic health parameters, it is likely that mitochondrial function in adipose tissue is a major factor that underlies the sex differences.

Our results have raised a number of questions. Are sex-specific differences well-conserved between species? In particular, do the differences in adipose mitochondrial function also occur in humans? It is clear that there exist major differences in adipose biology between sexes in humans (Karastergiou et al., 2013). A study of 732 members of 154 nuclear families found that adipose resting energy expenditure was significantly higher in women than men. These authors then examined gene expression in subcutaneous adipose in a separate cohort as well as a subset of their cohort and observed higher expression of genes involved in mitochondrial function, including UCP1, in women than men, similar to our findings in mice (Nookaew et al., 2013). How do liver and adipose differ in epigenetic organization in sexual development (Ghahramani et al., 2014; McCarthy et al., 2017) and when do these organizational changes occur in development? Also, are cardio-metabolic traits unusual in the degree of sex-dependent effects? While our work adds insight into the depth and breadth of sex differences in metabolism, it also emphasizes the relative lack of understanding of the biology underlying these differences. Previously, we have proposed as a long-term goal the development of a biologic network model that describes the differences between males and females (the “sexome”) on a system level (Arnold and Lusis, 2012). Such a model will require identifying the primary and downstream sex-biased factors that act on the network and how the sex-biased network interactions give rise to sex differences in the emergent phenotypes. We believe that our results provide compelling evidence as to why males and females in biological research should be treated as distinct organisms as a whole, rather than attempting to reconcile these differences one molecule at a time.

Limitations

Our study has several limitations. The mechanistic studies were limited to liver and adipose, and the role of estrogen was not explored. Although some evidence, discussed above, suggests that humans exhibit sexual dimorphisms for mitochondrial function, we did not directly test this.

STAR METHODS

CONTACT FOR REAGENT AND RESOURCE SHARING

Further information and requests for resources and reagents should be directed to and will be fulfilled by the Lead Contact, Aldons J. Lusis (jlusis@mednet.ucla.edu).

EXPERIMENTAL MODEL AND SUBJECT DETAILS

Animals—All of the mice strains included in the HMDP study were obtained from The Jackson Laboratory and have been described in detail (Bennett et al., 2010). The strains of

mice included in this study is listed in Table S2. The experimental design of the HF/HS feeding study has been described previously (Parks et al., 2013). Briefly, the mice were maintained on a chow diet (Ralston Purina Company) until 8 weeks of age before switching to a HF/HS (Research DietD12266B, New Brunswick, NJ) diet for 8 weeks. The gonadectomy and ovariectomy study is described in detail (Parks et al., 2015). The mice were either maintained on chow diet for 16 w or on chow diet until 8 weeks of age, or then switched to a HF/HS diet for 8 weeks. The mice were gonadectomized, gonadectomized with testosterone implantation, or sham operated under isoflurane anesthesia at 6 weeks of age. Mice were housed in rooms with a 14-hr light/10-hr dark cycle (light is on between 6 a.m. and 8 p.m.) at a temperature of 25 degrees. On the day of experiment, mice from both studies were sacrificed after a 4 h fast between 10.30 a.m. and noon. We did not assess the reproductive phase of the females as this was not feasible in such a large study. In mice that received hormonal replacement at time of surgery, a small incision was made at the base of the back of the neck. A 5 mg pellet of 5adihydrotestosterone 90-day release (innovative Research of America, FL) was inserted and the incision closed.

Principle component analysis was performed on gonadectamized liver samples using prcomp (R Studio). The contribution of each gene to total variances for principle components 1 and 2 were obtained and shown on Figure S3. To ask whether the observed shifts in male liver along the PC axes following gonadectomy in Figure 5B were due to the presence of the hormone itself, gonadectamized males were administered testosterone (DHT) or vehicle. Gene expression from the top drivers of PC1 were measured in liver using qPCR (Fig. 5) and compared between groups. Of the seven top contributing genes measured, 5 were significantly reversed upon hormone administration. These data suggest that the total shifts in liver gene expression following gonadectomy were substantially impacted by testosterone levels.

This study was performed in strict accordance with the recommendations in the Guide for the Care and Use of Laboratory Animals of the National Institutes of Health. All of the animals were handled according to approved institutional animal care and use committee (IACUC) protocols (#92–169) of the University of California at Los Angeles. The animal procedures were approved by the Institutional Care and Use Committee at University of California, Los Angeles.

METHOD DETAILS

Phenotype-phenotype correlations—Since the HMDP mice differ in size, it is likely that many metabolic measurements could simply reflect such differences. To correct for this, we have adjusted phenotypes using kidney weight, which tends to be relatively invariant among the strains.

For every pairwise combination of phenotypes, in each sex, we calculated biweight midcorrelation (a robust, and less sensitive to outliers, alternative to Pearson correlation) using bicorAndPvalue function of the WGCNA package. In addition to the theoretical p-value returned by the bicorAndPvalue, we performed 1000 permutations of each phenotype pair (total of 1,682,000 permutations). The male and female cross phenotype correlation matrix was visualized with R function ‘pheatmap’.

RNA Library preparation and sequencing—Upon sacrifice, tissues were instantly frozen in liquid nitrogen. Frozen tissues were homogenized in Qiazol, and following chloroform phase separation RNA was prepared from the pink phase using Qiagen miRNAeasy kits as per original protocol. Total RNA quality was validated with BioANAlyzer (all samples had RIN>8). Global gene expression in liver and gonadal adipose tissue from the HMDP strains were analyzed using Affymetrix HT_MG430A arrays, and data were filtered as described (Parks et al., 2013). RNA libraries were prepared by the sequencing facility at the UCLA Neurosciences Genomics Core using Illumina TruSeq Stranded kits v2 and paired-end sequencing. Reads were aligned using STAR 2.5.2b, mm10 genome and GENCODE M11 transcript annotation. First, we built a genome index that included the transcript annotation with k-mers adjusted to read length −1 (as suggested by STAR manual). Mapping was performed with 48Gb of RAM, and 12 processors. Reads-per-gene tables were generated as part of STAR output (https://github.com/alexdobin/STAR) and DESeq2 (https://bioconductor.org/packages/release/bioc/html/DESeq2.html) was used for differential expression analysis. Differential expression analysis was run in a multi-variate mode on each tissue separately, testing for both sex and diet effects. Plotting of PCA was carried out directly as part of DESeq2 analysis using “plotPCA” function.

Tissue Deconvolution—Cell composition of adipose was assessed by deconvolution using gene expression data from the HMDP or gonadectomy studies with SaVanT (http://newpathways.mcdb.ucla.edu/savant) using cell type signatures from the Human Primary Cell Atlas.

Heritability—Heritabilities and their standard errors were calculated using the software package GCTA (Genome-wide Complex Trait Analysis) (Yang et al., 2011). The source code for the version we used is publicly available at http://cnsgenomics.com/software/gcta/gcta_1.26.0_src.zip.

Genome-wide association analyses—Association analysis is a method of determining which regions of the genome have effects on a quantitative trait. In a panel of inbred mice such as the HMDP, the shared ancestry of many of the strains used results in population structure. A naïve approach to association analysis would ignore this structure and produce artificially low p-values since the contribution of the shared genetic background to the phenotypic values would mistakenly be attributed to the particular variant being tested for association. Therefore, mapping of each trait in each sex was performed using Fast-LMM (Factored spectrally-transformed Linear Mixed Models) with correction for population structure as previously described (Hasin-Brumshtein et al., 2016; Orozco et al., 2012; Parks et al., 2015). The regression equation used in this method includes a term that accounts for the genetic relatedness of all the individuals tested. The genetic relatedness matrix (GRM) is constructed from all of the SNPs tested, with the refinement that when testing SNPs on a particular chromosome N for association, all SNPs from chromosome N are excluded from the GRM. This prevents any SNP from incorrectly being used in the regression equation twice, which would result in potential false negative results. SNPs with minor allele frequencies below 5% or missing genotype frequencies greater than 10 % were excluded,

leaving approximately 200,000 SNPs (Rau et al., 2015) used in the final analysis. Genotypes for these SNPs were obtained using the Mouse Diversity Array (Yang et al., 2009).

***Lyplal1* studies—**Sperm from *Lyplal1*$^{tm1a(KOMP)Wtsi}$ C57BL/6N mice were obtained from the University of California Davis KOMP Repository Knockout Mouse Project and mice were rederived at University of California Los Angeles. Female and male mice were maintained on a chow diet (Ralston Purina Company) until 8 weeks of age when they were given a HF/HS diet (Research Diets-D12266B, New Brunswick, NJ) with the following composition: 16.8% kcal protein, 51.4% kcal carbohydrate, 31.8% kcal fat. Total body fat mass and lean mass were measured by magnetic resonance imaging using Bruker Minispec before the start of the HF/HS diet and thereby biweekly, as described (Parks et al., 2013). After 8 weeks on the HF/HS diet, mice were sacrificed after a 4-hr fast. Blood was collected by retro-orbital bleeding under isoflurane anesthesia. Subcutaneous, mesenteric, retroperitoneal and gonadal adipose tissues were carefully dissected and weighed from a subset of the animals. Plasma, liver and adipose tissues were frozen immediately after dissection in liquid nitrogen and stored at −80°C until analysis.

Mitochondrial DNA content—Mitochondrial DNA content was measured as described previously (Rooney et al., 2015; Venegas and Halberg, 2012; Vergnes et al., 2011). Briefly, total (mitochondrial and nuclear) DNA from gonadal adipose tissue was isolated by phenol/chloroform/isoamyl alcohol extraction. Both mitochondrial and nuclear DNA were amplified by quantitative PCR with 25 ng of total DNA using primers in the D-loop region (AATCTACCATCCTCCGTGAAACC; TCAGTTTAGCTACCCCCAAGTTTAA) and Tert gene (CTAGCTCATGTGTCAAGACCCTCTT; GCCAGCACGTTTCTCTCGTT), respectively. Mitochondrial DNA content, normalized to nuclear DNA, was calculated using the equation $2\ X\ 2^{-\Delta Ct}$ (ΔCt = D-loop Ct –Tert Ct) and then reported as relative units of corresponding female groups.

Mitochondrial bioenergetics—Mitochondria were isolated from fresh tissues and immediately used in an XF24 Analyzer (Seahorse Bioscience) as previously described (Vergnes et al., 2016). Briefly, the mitochondrial pellet was isolated by dual centrifugation at 800g and 8000g. 25 μg mitochondria were seeded per well by centrifugation. Oxygen consumption rate (OCR) was measured in the presence of 10 mM succinate (complex II substrate) and 2 μM rotenone (complex I inhibitor), and after sequential addition of 4 mM ADP (Complex V substrate), 2.5 μg/ml oligomycin (Complex V inhibitor), 4 μM FCCP (mitochondrial uncoupler) and 4 μM antimycin A (Complex III inhibitor). OCR was normalized per μg mitochondrial protein. Maximal respiration represents the response to FCCP. Coupled and uncoupled respiration rates were the oligomycin-sensitive and the difference between rates observed after the addition of oligomycin and antimycin A, respectively.

Mitochondrial immunoblot procedures and analyses of function—Mitochondria prepared for mitochondria bioenergetics as described above were lysed in Whole Cell Extraction buffer (WCE) containing 62.5mM Tris-HCl (pH 6.8), 2% (wt/v) Sodium dodecyl sulfate, and 10% glycerol (Seldin et al., 2017). Samples were then heated and diluted 1:5 in

water, and protein content measured using a BCA protein assay kit (Pierce). 10 ug samples were denatured in 4x LDS loading buffer (Life Technologies) with 10x reducing agent (Life Technologies) at 99°C for 20min, loaded at 10uL/well into 4–12% Bis-Tris gels (Invitrogen) and separated out at 130 volts for 2hr. Protein was then transferred to PVDF membranes (Immobilon) for 1.5hr at 35 volts. Following transfer, membranes were washed with TBST, and then blocked in 5% skim milk (Gibco) in TBST for 1hr at room temperature. Membranes were then placed in a primary antibody cocktail for total OxPhos complex cocktail (Abcam, # ab110413, 1:2000) or TOM20 (Santa Cruz, # sc-17764 1:500) on a shaker overnight at 4°C. The following day, membranes were washed 3X in TBST then placed in secondary antibodies (1:2000) for 1hr at room temperature. Blots were then washed 3X in TBST and placed in Amersham ECL detection solution (GE health sciences). Blots were imaged using IMAGER and bands were quantified using Image J Software.

Immunohistochemistry—Gonadal fat samples were dissected and subsequently fixed and stored in 4% paraformaldehyde. After dehydration, tissues were embedded in paraffin and cut into 5 μm slices. Immunohistochemical staining was performed on a Discovery XT automated stainer (Ventana, Medical Systems) using rabbit anti-UCP1 antibody (1:1500; ab10983, Abcam). Signal detection was performed using the diaminobenzidine as a chromogen (Ventana Medical Systems). Images obtained by UCP1 and H&E staining were analyzed using the commercially available image analysis software Definiens Developer XD2.1 (Definiens AG; München, Germany). For this purpose, all stained slides were scanned at 20× objective magnification using a Mirax Desk digital slide scanner (Carl Zeiss MicroImaging, Munich, Germany), and the resulting images were imported into image analysis software. A specific rule set was defined to detect the stained tissue area (UCP1) or the adipocytes (H&E) within each defined region. The quantified parameter was the percentage of the UCP1 stained area related to the defined tissue area. For H&E staining the calculated parameter was the mean size of the adipocytes.

QUANTIFICATION AND STATISTICAL ANALYSIS

Statistical Analyses—Phenotype-phenotype correlations: Correlations were calculated in R with bicor function from WGCNA (https://cran.r-project.org/web/packages/WGCNA/index.html). Bicor calculates biweight mid-correlations, which are a robust (less sensitive to outliers) alternative to Pearson correlations. Permutations were carried out in R, by randomizing one of the phenotypes, then calculating the p-value and correlation on the permuted data. For each phenotype-phenotype pair we obtained 1000 randomized p values. Distributions of randomized p-values were very similar between all pairs of phenotypes, thus we used the combined distributions of p-values to assess significance thresholds.

Microarrays: gene expression in adipose and liver of HMDP mice was measured with microarrays, as described in Parks et al., 2013. Array data was normalized and adjusted for batch effects using RMA - a standard processing package for Affymetrix microarray data. Outlier samples (one in adipose and one in liver) and strains that were not present in all 4 data-sets were removed from further analysis. We then filtered out: 1. Low quality probes, as annotated in Affymetrix annotation file HT_MG-430A.na36.annot.csv (downloaded from company website). 2. Low expressed probes: we required expression >4 in 70 or more

strains in either sex. Differential expression analysis was carried out with R package "limma" (http://bioconductor.org/packages/limma/) at the probe level, using design model of ~strain+ sex.

Gene enrichment analysis was carried out using DAVID (https://david.ncifcrf.gov/). For background expression we used tissue specific list of expressed genes, the same as was used with for differential expression. The threshold for significance was $p<0.01$. Unless otherwise noted, values presented are expressed as means ± SEM. The two-sample Student's t-test was used to examine the difference between the two groups. All analyses were performed using R 3.1.0 (Vienna, Austria), and p-values <0.05 were considered statistically significant.

The statistical parameters can also be found in the figure legends

Data and Software Availability: The expression arrays and RNA-Seq data used in this study are listed below:

HMDP expression arrays (liver and adipose)	NCBI GEO	GSE64770
Gonadectomized RNA-seq data	NCBI GEO	GSE112947

Supplementary Material

Refer to Web version on PubMed Central for supplementary material.

Acknowledgements

We thank Sarada Charugundla for plasma metabolite analysis, and Yonghong Meng for immunoblot analysis. We also thank Sebastian Cucuruz and Cynthia Striese from the Helmholtz Center for scanning the UCP-1 and Caspase 3 immuno-staining.

This work was supported by the National Institutes of Health Grants HL28481, HL30568, K99-HL138193, T32-HL69766, T32-HL007895 and R00-HL123021, Transatlantic Network of Excellence Award 12CVD02, The Research Council of Norway (240405/F20), the Helmholtz Alliance ICEMED (Imaging and Curing Environmental Metabolic Diseases), the Network Fund of the Helmholtz Association, the German Center for Diabetes Research (DZD) and the American Heart Association (AHA) fellowship 18POST33990256, and Project A4 (PI S.M. Hofmann) of the SFB1123 from the German Research Foundation (DFG).

References

Afshari NA, Igo RP, Jr., Morris NJ, Stambolian D, Sharma S, Pulagam VL, Dunn S, Stamler JF, Truitt BJ, Rimmler J, et al. (2017). Genome-wide association study identifies three novel loci in Fuchs endothelial corneal dystrophy. Nature communications 8, 14898.

Andreux PA, Williams EG, Koutnikova H, Houtkooper RH, Champy MF, Henry H, Schoonjans K, Williams RW, and Auwerx J (2012). Systems genetics of metabolism: the use of the BXD murine reference panel for multiscalar integration of traits. Cell 150, 1287–1299. [PubMed: 22939713]

Arnold AP (2009). The organizational-activational hypothesis as the foundation for a unified theory of sexual differentiation of all mammalian tissues. Hormones and behavior 55, 570–578. [PubMed: 19446073]

Arnold AP (2017). A general theory of sexual differentiation. Journal of neuroscience research 95, 291–300. [PubMed: 27870435]

Arnold AP, and Lusis AJ (2012). Understanding the sexome: measuring and reporting sex differences in gene systems. Endocrinology 153, 2551–2555. [PubMed: 22434084]

Bellott DW, Hughes JF, Skaletsky H, Brown LG, Pyntikova T, Cho TJ, Koutseva N, Zaghlul S, Graves T, Rock S, et al. (2014). Mammalian Y chromosomes retain widely expressed dosage-sensitive regulators. Nature 508, 494–499. [PubMed: 24759411]

Bennett BJ, Farber CR, Orozco L, Kang HM, Ghazalpour A, Siemers N, Neubauer M, Neuhaus I, Yordanova R, Guan B, et al. (2010). A high-resolution association mapping panel for the dissection of complex traits in mice. Genome research 20, 281–290. [PubMed: 20054062]

Bouret SG (2013). Organizational actions of metabolic hormones. Frontiers in neuroendocrinology 34, 18–26. [PubMed: 23357643]

Byers SL, Wiles MV, Dunn SL, and Taft RA (2012). Mouse estrous cycle identification tool and images. PLoS One 7, e35538. [PubMed: 22514749]

Cannon B, and Nedergaard J (2004). Brown adipose tissue: function and physiological significance. Physiological reviews 84, 277–359. [PubMed: 14715917]

Capel B (2017). Vertebrate sex determination: evolutionary plasticity of a fundamental switch. Nature reviews. Genetics 18, 675–689.

Castagne R, Zeller T, Rotival M, Szymczak S, Truong V, Schillert A, Tregouet DA, Munzel T, Ziegler A, Cambien F, et al. (2011). Influence of sex and genetic variability on expression of X-linked genes in human monocytes. Genomics 98, 320–326. [PubMed: 21763416]

Charlesworth B (1996). The evolution of chromosomal sex determination and dosage compensation. Current biology : CB 6, 149–162. [PubMed: 8673462]

Chen H, Cade BE, Gleason KJ, Bjonnes AC, Stilp AM, Sofer T, Conomos MP, Ancoli-Israel S, Arens R, Azarbarzin A, et al. (2017). Multi-ethnic Meta-analysis Identifies RAI1 as a Possible Obstructive Sleep Apnea Related Quantitative Trait Locus in Men. American journal of respiratory cell and molecular biology.

Chen X, McClusky R, Chen J, Beaven SW, Tontonoz P, Arnold AP, and Reue K (2012). The number of x chromosomes causes sex differences in adiposity in mice. PLoS genetics 8, e1002709. [PubMed: 22589744]

Choi Y, and Chan AP (2015). PROVEAN web server: a tool to predict the functional effect of amino acid substitutions and indels. Bioinformatics (Oxford, England) 31, 2745–2747.

Della Torre S, Mitro N, Meda C, Lolli F, Pedretti S, Barcella M, Ottobrini L, Metzger D, Caruso D, and Maggi A (2018). Short-Term Fasting Reveals Amino Acid Metabolism as a Major Sex-Discriminating Factor in the Liver. Cell Metab 28, 256–267 e255. [PubMed: 29909969]

Dimas AS, Nica AC, Montgomery SB, Stranger BE, Raj T, Buil A, Giger T, Lappalainen T, Gutierrez-Arcelus M, Mu TC, et al. (2012). Sex-biased genetic effects on gene regulation in humans. Genome research 22, 2368–2375. [PubMed: 22960374]

Disteche CM (2012). Dosage compensation of the sex chromosomes. Annual review of genetics 46, 537–560.

Dobner J, Ress C, Rufinatscha K, Salzmann K, Salvenmoser W, Folie S, Wieser V, Moser P, Weiss G, Goebel G, et al. (2017). Fat-enriched rather than high-fructose diets promote whitening of adipose tissue in a sex-dependent manner. The Journal of nutritional biochemistry 49, 22–29. [PubMed: 28863366]

Falls JG, Ryu DY, Cao Y, Levi PE, and Hodgson E (1997). Regulation of mouse liver Flavin-containing monooxygenases 1 and 3 by sex steroids. Arch Biochem Biophys 342, 212–223. [PubMed: 9186481]

Fields CT, Chassaing B, Paul MJ, Gewirtz AT, and de Vries GJ (2017). Vasopressin deletion is associated with sex-specific shifts in the gut microbiome. Gut microbes, 1–13.

Fox CS, Liu Y, White CC, Feitosa M, Smith AV, Heard-Costa N, Lohman K, Johnson AD, Foster MC, Greenawalt DM, et al. (2012). Genome-wide association for abdominal subcutaneous and visceral adipose reveals a novel locus for visceral fat in women. PLoS genetics 8, e1002695. [PubMed: 22589738]

Ghahramani NM, Ngun TC, Chen PY, Tian Y, Krishnan S, Muir S, Rubbi L, Arnold AP, de Vries GJ, Forger NG, et al. (2014). The effects of perinatal testosterone exposure on the DNA methylome of the mouse brain are late-emerging. Biology of sex differences 5, 8. [PubMed: 24976947]

Giordano A, Frontini A, and Cinti S (2016). Convertible visceral fat as a therapeutic target to curb obesity. Nature reviews. Drug discovery 15, 405–424. [PubMed: 26965204]

Gregg C, Zhang J, Butler JE, Haig D, and Dulac C (2010). Sex-specific parent-of-origin allelic expression in the mouse brain. Science 329, 682–685. [PubMed: 20616234]

Hager R, Cheverud JM, Leamy LJ, and Wolf JB (2008). Sex dependent imprinting effects on complex traits in mice. BMC evolutionary biology 8, 303. [PubMed: 18976474]

Hasin-Brumshtein Y, Khan AH, Hormozdiari F, Pan C, Parks BW, Petyuk VA, Piehowski PD, Brummer A, Pellegrini M, Xiao X, et al. (2016). Hypothalamic transcriptomes of 99 mouse strains reveal trans eQTL hotspots, splicing QTLs and novel non-coding genes. Elife 5.

Heid IM, Jackson AU, Randall JC, Winkler TW, Qi L, Steinthorsdottir V, Thorleifsson G, Zillikens MC, Speliotes EK, Magi R, et al. (2010). Meta-analysis identifies 13 new loci associated with waist-hip ratio and reveals sexual dimorphism in the genetic basis of fat distribution. Nature genetics 42, 949–960. [PubMed: 20935629]

Jalouli M, Carlsson L, Ameen C, Linden D, Ljungberg A, Michalik L, Eden S, Wahli W, and Oscarsson J (2003). Sex difference in hepatic peroxisome proliferator-activated receptor alpha expression: influence of pituitary and gonadal hormones. Endocrinology 144, 101–109. [PubMed: 12488335]

Karastergiou K, Fried SK, Xie H, Lee MJ, Divoux A, Rosencrantz MA, Chang RJ, and Smith SR (2013). Distinct developmental signatures of human abdominal and gluteal subcutaneous adipose tissue depots. The Journal of clinical endocrinology and metabolism 98, 362–371. [PubMed: 23150689]

Karp NA, Mason J, Beaudet AL, Benjamini Y, Bower L, Braun RE, Brown SDM, Chesler EJ, Dickinson ME, Flenniken AM, et al. (2017). Prevalence of sexual dimorphism in mammalian phenotypic traits. Nature communications 8, 15475.

Kenney-Hunt JP, Wang B, Norgard EA, Fawcett G, Falk D, Pletscher LS, Jarvis JP, Roseman C, Wolf J, and Cheverud JM (2008). Pleiotropic patterns of quantitative trait loci for 70 murine skeletal traits. Genetics 178, 2275–2288. [PubMed: 18430949]

Kim SN, Jung YS, Kwon HJ, Seong JK, Granneman JG, and Lee YH (2016). Sex differences in sympathetic innervation and browning of white adipose tissue of mice. Biology of sex differences 7, 67. [PubMed: 27990249]

Krohn J, Speed D, Palme R, Touma C, Mott R, and Flint J (2014). Genetic interactions with sex make a relatively small contribution to the heritability of complex traits in mice. PLoS One 9, e96450. [PubMed: 24811081]

Kukurba KR, Parsana P, Balliu B, Smith KS, Zappala Z, Knowles DA, Fave MJ, Davis JR, Li X, Zhu X, et al. (2016). Impact of the X Chromosome and sex on regulatory variation. Genome research 26, 768–777. [PubMed: 27197214]

Kwekel JC, Vijay V, Han T, Moland CL, Desai VG, and Fuscoe JC (2017). Sex and age differences in the expression of liver microRNAs during the life span of F344 rats. Biology of sex differences 8, 6. [PubMed: 28174625]

Kwon YC, Kim JJ, Yun SW, Yu JJ, Yoon KL, Lee KY, Kil HR, Kim GB, Han MK, Song MS, et al. (2017). Male-specific association of the FCGR2A His167Arg polymorphism with Kawasaki disease. PLoS One 12, e0184248. [PubMed: 28886140]

Lindgren CM, Heid IM, Randall JC, Lamina C, Steinthorsdottir V, Qi L, Speliotes EK, Thorleifsson G, Willer CJ, Herrera BM, et al. (2009). Genome-wide association scan metaanalysis identifies three Loci influencing adiposity and fat distribution. PLoS genetics 5, e1000508. [PubMed: 19557161]

Link JC, Chen X, Arnold AP, and Reue K (2013). Metabolic impact of sex chromosomes. Adipocyte 2, 74–79. [PubMed: 23805402]

Link JC, and Reue K (2017). Genetic Basis for Sex Differences in Obesity and Lipid Metabolism. Annual review of nutrition 37, 225–245.

Liu CT, Estrada K, Yerges-Armstrong LM, Amin N, Evangelou E, Li G, Minster RL, Carless MA, Kammerer CM, Oei L, et al. (2012a). Assessment of gene-by-sex interaction effect on bone mineral density. Journal of bone and mineral research : the official journal of the American Society for Bone and Mineral Research 27, 2051–2064.

Liu LY, Schaub MA, Sirota M, and Butte AJ (2012b). Sex differences in disease risk from reported genome-wide association study findings. Human genetics 131, 353–364. [PubMed: 21858542]

Lovejoy JC, Sainsbury A, and Stock Conference Working G. (2009). Sex differences in obesity and the regulation of energy homeostasis. Obesity reviews : an official journal of the International Association for the Study of Obesity 10, 154–167. [PubMed: 19021872]

Lu S, Zhao LJ, Chen XD, Papasian CJ, Wu KH, Tan LJ, Wang ZE, Pei YF, Tian Q, and Deng HW (2017). Bivariate genome-wide association analyses identified genetic pleiotropic effects for bone mineral density and alcohol drinking in Caucasians. Journal of bone and mineral metabolism 35, 649–658. [PubMed: 28012008]

Lusis AJ, Seldin MM, Allayee H, Bennett BJ, Civelek M, Davis RC, Eskin E, Farber CR, Hui S, Mehrabian M, et al. (2016). The Hybrid Mouse Diversity Panel: a resource for systems genetics analyses of metabolic and cardiovascular traits. Journal of lipid research 57, 925–942. [PubMed: 27099397]

McCarthy MM, Auger AP, Bale TL, De Vries GJ, Dunn GA, Forger NG, Murray EK, Nugent BM, Schwarz JM, and Wilson ME (2009). The epigenetics of sex differences in the brain. The Journal of neuroscience : the official journal of the Society for Neuroscience 29, 12815–12823. [PubMed: 19828794]

McCarthy MM, Nugent BM, and Lenz KM (2017). Neuroimmunology and neuroepigenetics in the establishment of sex differences in the brain. Nature reviews. Neuroscience 18, 471–484. [PubMed: 28638119]

Melo JA, Shendure J, Pociask K, and Silver LM (1996). Identification of sex-specific quantitative trait loci controlling alcohol preference in C57BL/ 6 mice. Nature genetics 13, 147–153. [PubMed: 8640219]

Mittelstrass K, Ried JS, Yu Z, Krumsiek J, Gieger C, Prehn C, Roemisch-Margl W, Polonikov A, Peters A, Theis FJ, et al. (2011). Discovery of sexual dimorphisms in metabolic and genetic biomarkers. PLoS genetics 7, e1002215. [PubMed: 21852955]

Mozhui K, Lu L, Armstrong WE, and Williams RW (2012). Sex-specific modulation of gene expression networks in murine hypothalamus. Frontiers in neuroscience 6, 63. [PubMed: 22593731]

Myers RA, Scott NM, Gauderman WJ, Qiu W, Mathias RA, Romieu I, Levin AM, PinoYanes M, Graves PE, Villarreal AB, et al. (2014). Genome-wide interaction studies reveal sex-specific asthma risk alleles. Human molecular genetics 23, 5251–5259. [PubMed: 24824216]

Nookaew I, Svensson PA, Jacobson P, Jernas M, Taube M, Larsson I, AnderssonAssarsson JC, Sjostrom L, Froguel P, Walley A, et al. (2013). Adipose tissue resting energy expenditure and expression of genes involved in mitochondrial function are higher in women than in men. The Journal of clinical endocrinology and metabolism 98, E370–378. [PubMed: 23264395]

Ober C, Loisel DA, and Gilad Y (2008). Sex-specific genetic architecture of human disease. Nature reviews. Genetics 9, 911–922.

Org E, Mehrabian M, Parks BW, Shipkova P, Liu X, Drake TA, and Lusis AJ (2016). Sex differences and hormonal effects on gut microbiota composition in mice. Gut microbes 7, 313–322. [PubMed: 27355107]

Orozco LD, Bennett BJ, Farber CR, Ghazalpour A, Pan C, Che N, Wen P, Qi HX, Mutukulu A, Siemers N, et al. (2012). Unraveling inflammatory responses using systems genetics and gene-environment interactions in macrophages. Cell 151, 658–670. [PubMed: 23101632]

Palmer BF, and Clegg DJ (2014). Oxygen sensing and metabolic homeostasis. Molecular and cellular endocrinology 397, 51–58. [PubMed: 25132648]

Parks BW, Nam E, Org E, Kostem E, Norheim F, Hui ST, Pan C, Civelek M, Rau CD, Bennett BJ, et al. (2013). Genetic control of obesity and gut microbiota composition in response to high-fat, high-sucrose diet in mice. Cell metabolism 17, 141–152. [PubMed: 23312289]

Parks BW, Sallam T, Mehrabian M, Psychogios N, Hui ST, Norheim F, Castellani LW, Rau CD, Pan C, Phun J, et al. (2015). Genetic architecture of insulin resistance in the mouse. Cell metabolism 21, 334–346. [PubMed: 25651185]

Randall JC, Winkler TW, Kutalik Z, Berndt SI, Jackson AU, Monda KL, Kilpelainen TO, Esko T, Magi R, Li S, et al. (2013a). Sex-stratified genome-wide association studies including 270,000

individuals show sexual dimorphism in genetic loci for anthropometric traits. PLoS genetics 9, e1003500. [PubMed: 23754948]

Randall JC, Winkler TW, Kutalik Z, Berndt SI, Jackson AU, Monda KL, Kilpelainen TO, Esko T, Magi R, Li S, et al. (2013b). Sex-stratified genome-wide association studies including 270,000 individuals show sexual dimorphism in genetic loci for anthropometric traits. PLoS genetics 9, e1003500. [PubMed: 23754948]

Rau CD, Parks B, Wang Y, Eskin E, Simecek P, Churchill GA, and Lusis AJ (2015). HighDensity Genotypes of Inbred Mouse Strains: Improved Power and Precision of Association Mapping. G3 5, 2021–2026. [PubMed: 26224782]

Rawlik K, Canela-Xandri O, and Tenesa A (2016). Evidence for sex-specific genetic architectures across a spectrum of human complex traits. Genome biology 17, 166. [PubMed: 27473438]

Rinn JL, Rozowsky JS, Laurenzi IJ, Petersen PH, Zou K, Zhong W, Gerstein M, and Snyder M (2004). Major molecular differences between mammalian sexes are involved in drug metabolism and renal function. Developmental cell 6, 791–800. [PubMed: 15177028]

Rinn JL, and Snyder M (2005). Sexual dimorphism in mammalian gene expression. Trends in genetics : TIG 21, 298–305. [PubMed: 15851067]

Rooney JP, Ryde IT, Sanders LH, Howlett EH, Colton MD, Germ KE, Mayer GD, Greenamyre TJ, and Meyer JN (2015). PCR Based Determination of Mitochondrial DNA Copy Number in Multiple Species. Methods in molecular biology (Clifton, N.J.) 1241, 23–38.

Roy AK, and Chatterjee B (1983). Sexual dimorphism in the liver. Annual review of physiology 45, 37–50.

Seldin MM, Kim ED, Romay MC, Li S, Rau CD, Wang JJ, Krishnan KC, Wang Y, Deb A, and Lusis AJ (2017). A systems genetics approach identifies Trp53inp2 as a link between cardiomyocyte glucose utilization and hypertrophic response. American journal of physiology. Heart and circulatory physiology 312, H728–H741. [PubMed: 28235788]

Silkaitis K, and Lemos B (2014). Sex-biased chromatin and regulatory cross-talk between sex chromosomes, autosomes, and mitochondria. Biology of sex differences 5, 2. [PubMed: 24422881]

Stubbins RE, Najjar K, Holcomb VB, Hong J, and Nunez NP (2012). Oestrogen alters adipocyte biology and protects female mice from adipocyte inflammation and insulin resistance. Diabetes, obesity & metabolism 14, 58–66.

Tai ES, bin Ali A, Zhang Q, Loh LM, Tan CE, Retnam L, El Oakley RM, and Lim SK (2003). Hepatic expression of PPARalpha, a molecular target of fibrates, is regulated during inflammation in a gender-specific manner. FEBS Lett 546, 237–240. [PubMed: 12832047]

Trabzuni D, Ramasamy A, Imran S, Walker R, Smith C, Weale ME, Hardy J, Ryten M, and North American Brain Expression, C. (2013). Widespread sex differences in gene expression and splicing in the adult human brain. Nature communications 4, 2771.

Traglia M, Bseiso D, Gusev A, Adviento B, Park DS, Mefford JA, Zaitlen N, and Weiss LA (2017). Genetic Mechanisms Leading to Sex Differences Across Common Diseases and Anthropometric Traits. Genetics 205, 979–992. [PubMed: 27974502]

van Nas A, Guhathakurta D, Wang SS, Yehya N, Horvath S, Zhang B, Ingram-Drake L, Chaudhuri G, Schadt EE, Drake TA, et al. (2009). Elucidating the role of gonadal hormones in sexually dimorphic gene coexpression networks. Endocrinology 150, 1235–1249. [PubMed: 18974276]

Varlamov O, Bethea CL, and Roberts CT, Jr. (2014). Sex-specific differences in lipid and glucose metabolism. Frontiers in endocrinology 5, 241. [PubMed: 25646091]

Venegas V, and Halberg MC (2012). Methods in Molecular Biology. Methods in molecular biology (Clifton, N.J.) 837, 327–335.

Ventura-Clapier R, Moulin M, Piquereau J, Lemaire C, Mericskay M, Veksler V, and Garnier A (2017). Mitochondria: a central target for sex differences in pathologies. Clinical science (London, England : 1979) 131, 803–822.

Vergnes L, Chin R, Young SG, and Reue K (2011). Heart-type Fatty Acid-binding Protein Is Essential for Efficient Brown Adipose Tissue Fatty Acid Oxidation and Cold Tolerance. Journal of Biological Chemistry 286, 380–390. [PubMed: 21044951]

Vergnes L, Davies GR, Lin JY, Yeh MW, Livhits MJ, Harari A, Symonds ME, Sacks HS, and Reue K (2016). Adipocyte Browning and Higher Mitochondrial Function in Periadrenal But Not SC Fat in Pheochromocytoma. The Journal of clinical endocrinology and metabolism 101, 4440–4448. [PubMed: 27575944]

Vieira Potter VJ, Strissel KJ, Xie C, Chang E, Bennett G, Defuria J, Obin MS, and Greenberg AS (2012). Adipose tissue inflammation and reduced insulin sensitivity in ovariectomized mice occurs in the absence of increased adiposity. Endocrinology 153, 4266–4277. [PubMed: 22778213]

Wang S, Yehya N, Schadt EE, Wang H, Drake TA, and Lusis AJ (2006). Genetic and genomic analysis of a fat mass trait with complex inheritance reveals marked sex specificity. PLoS genetics 2, e15. [PubMed: 16462940]

Watson RA, Gates AS, Wynn EH, Calvert FE, Girousse A, Lelliott CJ, and Barroso I (2017). Lyplal1 is dispensable for normal fat deposition in mice. Disease models & mechanisms 10, 1481–1488. [PubMed: 29084768]

Weiss LA, Pan L, Abney M, and Ober C (2006). The sex-specific genetic architecture of quantitative traits in humans. Nature genetics 38, 218–222. [PubMed: 16429159]

White UA, and Tchoukalova YD (2014). Sex dimorphism and depot differences in adipose tissue function. Biochimica et biophysica acta 1842, 377–392. [PubMed: 23684841]

Wu Y, Lee MJ, Ido Y, and Fried SK (2017). High-fat diet-induced obesity regulates MMP3 to modulate depot- and sex-dependent adipose expansion in C57BL/6J mice. American journal of physiology. Endocrinology and metabolism 312, E58–E71. [PubMed: 27879248]

Yang H, Ding Y, Hutchins LN, Szatkiewicz J, Bell TA, Paigen BJ, Graber JH, de Villena FP, and Churchill GA (2009). A customized and versatile high-density genotyping array for the mouse. Nature methods 6, 663–666. [PubMed: 19668205]

Yang J, Lee SH, Goddard ME, and Visscher PM (2011). GCTA: a tool for genome-wide complex trait analysis. American journal of human genetics 88, 76–82. [PubMed: 21167468]

Yang X, Schadt EE, Wang S, Wang H, Arnold AP, Ingram-Drake L, Drake TA, and Lusis AJ (2006). Tissue-specific expression and regulation of sexually dimorphic genes in mice. Genome research 16, 995–1004. [PubMed: 16825664]

Yao C, Joehanes R, Johnson AD, Huan T, Esko T, Ying S, Freedman JE, Murabito J, Lunetta KL, Metspalu A, et al. (2014). Sex- and age-interacting eQTLs in human complex diseases. Human molecular genetics 23, 1947–1956. [PubMed: 24242183]

Highlights

- Sex differences in phenotype and gene expression depend upon genetic background
- The gene *Lypla1* impacts obesity in a sex-specific manner
- Functional analyses reveal sex differences for adipose tissue beiging
- Adipose mitochondrial function depends upon gene-by-sex interactions

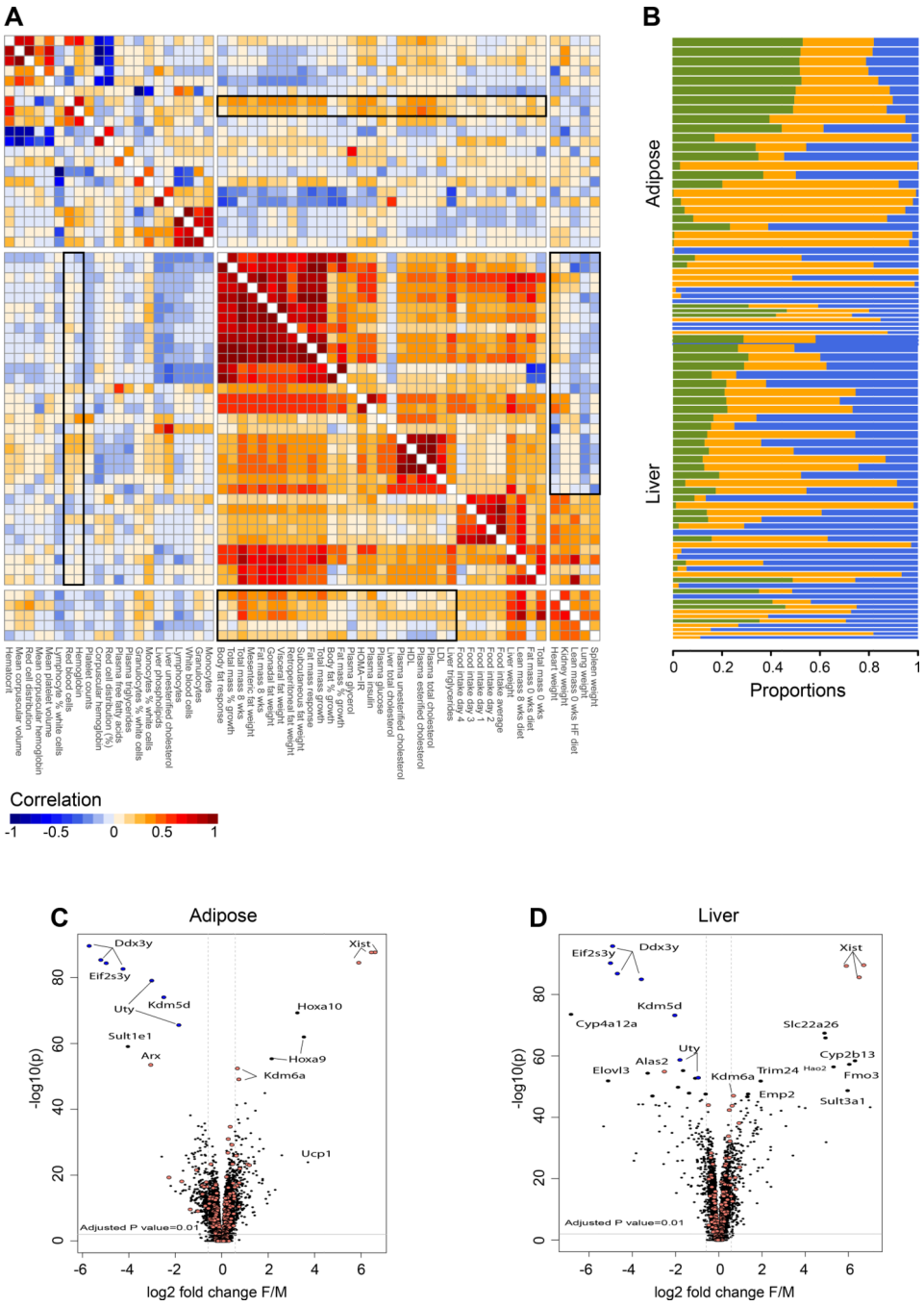

Figure 1. Cardio-metabolic traits exhibit sex-specific interdependencies in trait-trait and traittranscript correlations.

A. Heatmap representing pairwise biweight mid-correlation between phenotypes in females (lower triangle) and males (upper triangle). Two areas of different correlation structure are highlighted with boxes. All HMDP strains for which the data were available have been included in this analysis. **B.** Proportion of overlap of transcripts associated ($p<10^{-6}$) with phenotypes in both sexes in liver and adipose. Green indicates proportion of overlapping genes, while orange and blue show sex specific associations for females and males

respectively. Bar width is proportional to log2 of number of genes associated with the trait in total (see Table S1 for phenotypes). **C,D** Volcano plots of sex differences in expression in hfHMDP in the adipose **C** and liver **D**. Horizontal grey lines indicate adjusted threshold of $p<0.01$, vertical grey lines indicate 2 fold difference. Genes residing on chromosomes X and Y are colored pink and blue, respectively.

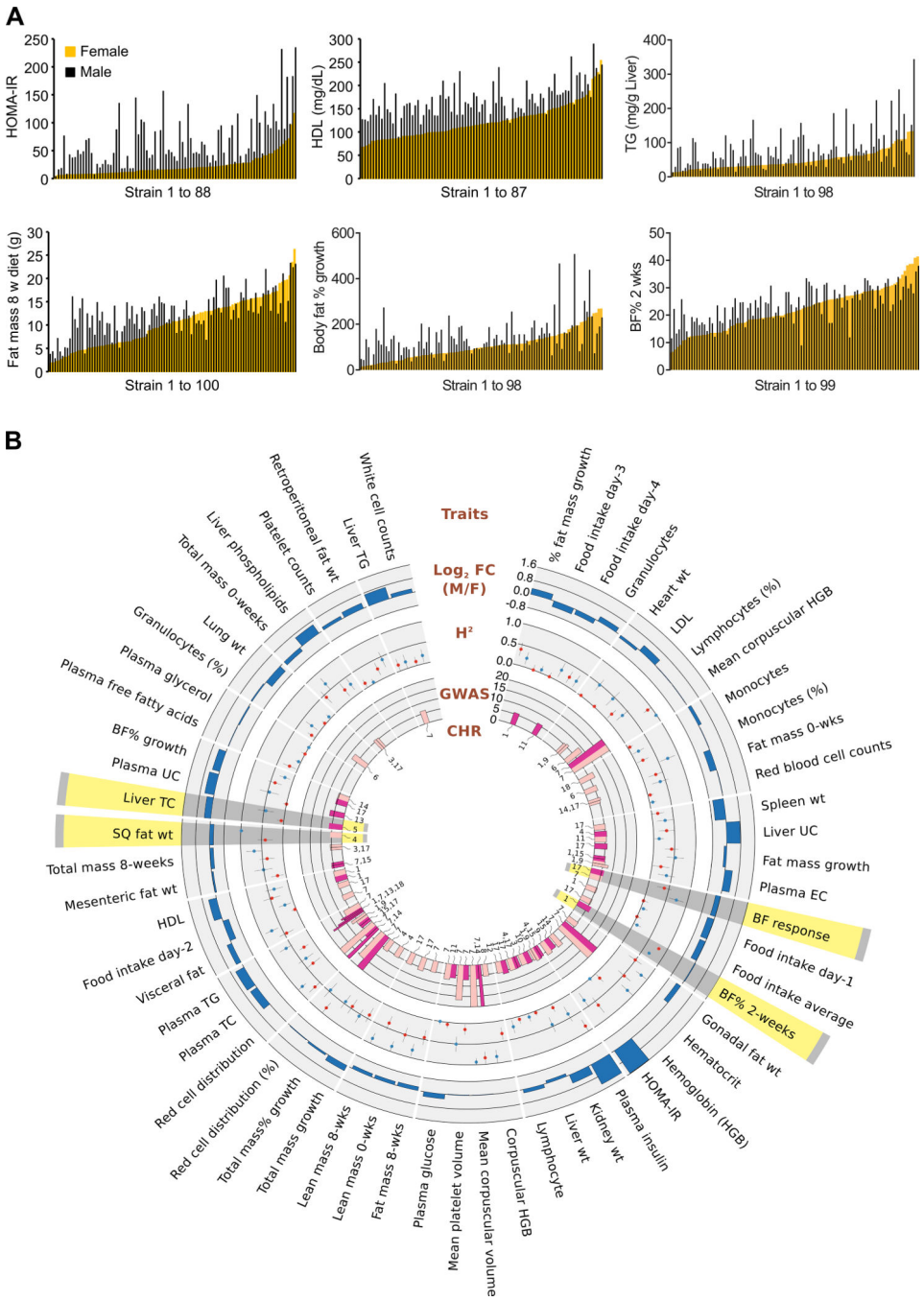

Figure 2. Sex differences in metabolic traits and their genetic architecture.

A. Six metabolic traits (HOMA-IR, HDL, plasma TG, fat mass, body fat % growth and body fat % after 2 weeks of diet) which exemplify gene by sex interaction. All phenotypes are rank ordered by female strains (orange). Male averages are in black. **B**. Circos plot showing an overview of sex-specific regulation of clinical traits. The outermost track (blue bars) show the relative log2 fold change (FC) across all strains (male vs. female). The middle track represents heritability estimates for the metabolic traits in females (red) and males (blue). Bars indicate 95% confidence interval. The innermost track represents -log10pvalue (capped

at 20) of notable GWAS loci in females (dark pink) and males (light pink), with their respective genome positions indicated below the bars. Bars indicate significant ($p<4.1\times10^{-6}$) mapping. Examples of sex-specific traits are highlighted and are discussed in detail in Figures 3 and 4.

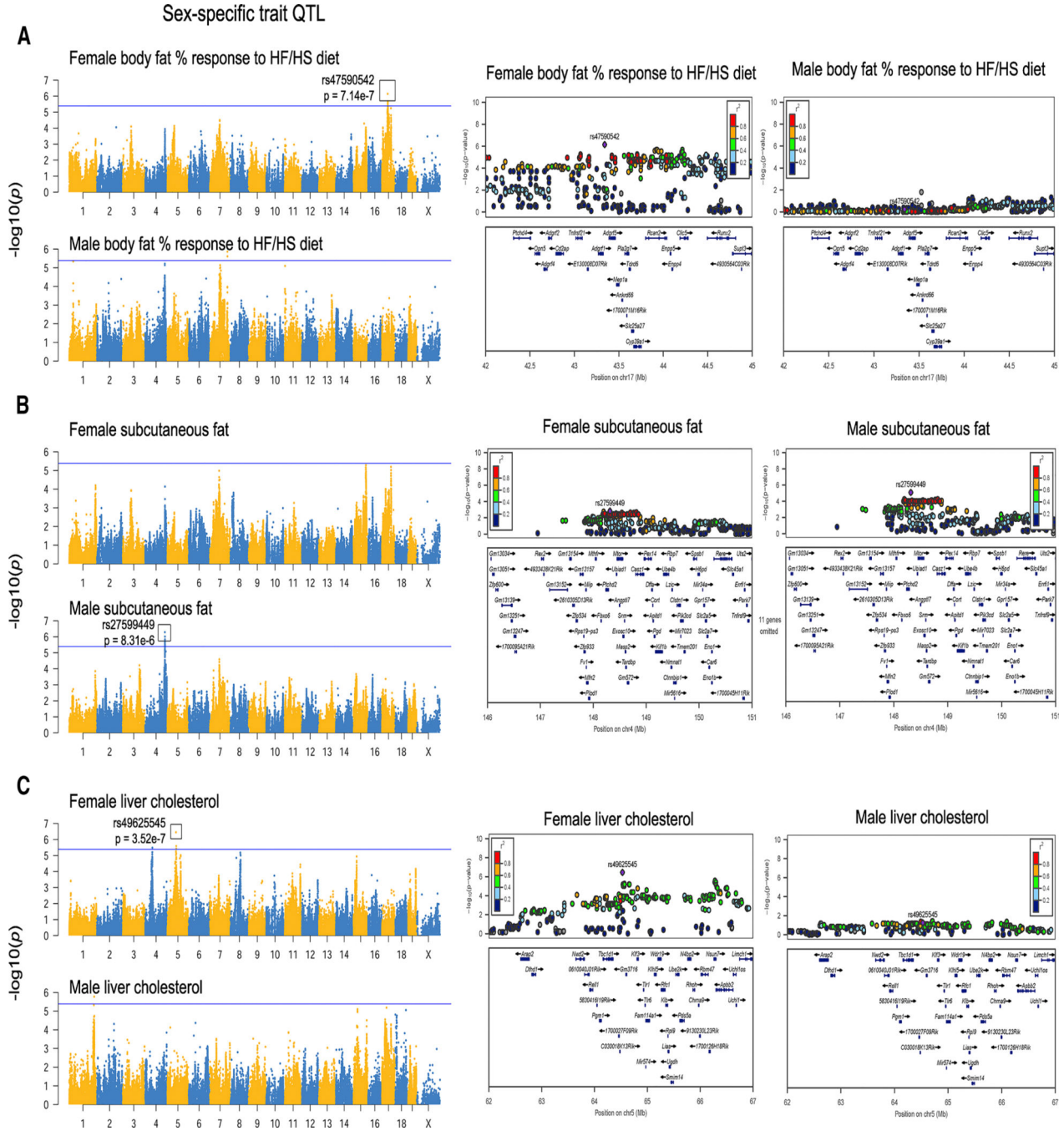

Figure 3. Sex-specific genetic loci for clinical traits

A-C. Examples of sex-specific genome-wide significant loci (left) and locuszoom plots for the indicated peak SNP in females (middle) or males (right). Bars indicate significant ($p<4.1\times10^{-6}$) mapping.

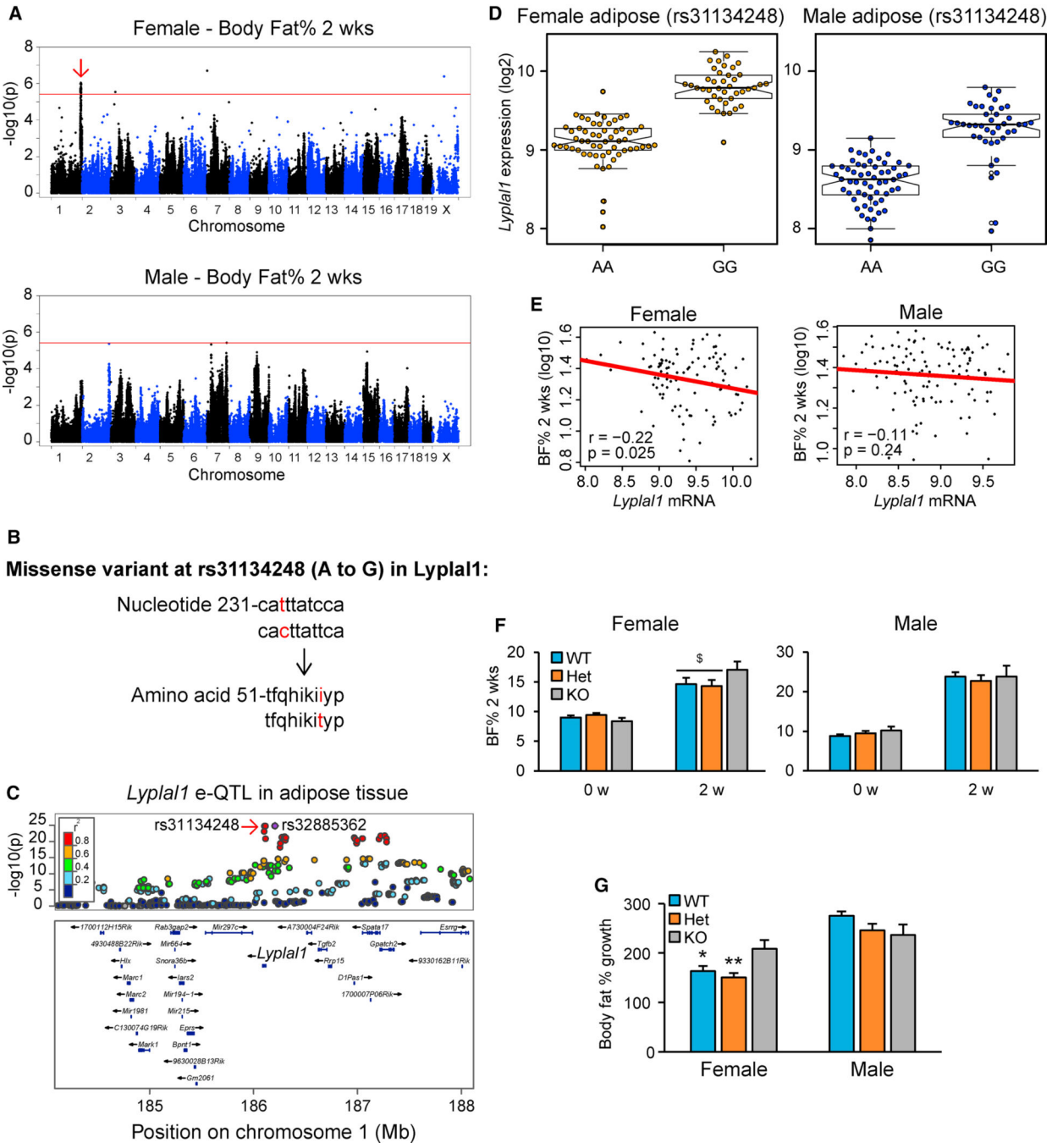

Figure 4. *Lyplal1* exhibits a sex-specific gene-by-diet effect on body fat % growth.

A. Manhattan plot showing the significance (−log10 of p value) of all SNPs and percent body fat percentage after 2 weeks of HF/HS feeding in female and male hfHMDP mice. Chr. 1 locus containing the *Lyplal1* gene is indicated with an arrow. The genome-wide significant threshold (red) of $p = 4.1\times10^{-6}$ is indicated. GWAS was performed on log10-transformed data to achieve a normal distribution **B.** Missense variant at rs31134248 (A to G) in the *Lyplal1* gene. The resulting changes in nucleotide and amino acid sequences are depicted in red letters. **C**. Locus zoom plot for cis-eQTL associations between *Lyplal1* expression and

the nearby SNPs at chr. 1. The significant association (–log10 of p value) between SNPs and *Lyplal1* are depicted. The degree of correlation between the SNP correlating the most with *Lyplal1* (rs3288536) and all other SNPs are shown. The missense variant (rs31134248) is depicted. **D**. *Lyplal1* expression in female and male adipose tissue in hfHMDP for the two missense alleles (rs31134248). **E**. Correlation of adipose gene expression of *Lyplal1* with body fat percentage after 2 weeks of HF/HS diet in female and male hfHMDP mice. **F** BF% both before and after 2 weeks of HF/HS diet in in female and male wild-type (WT), heterozygotes (Het) and KO mice for *Lyplal1*. **G** BF% growth (0 to 2 weeks) in response to a HF/HS diet in female and male WT, Het and KO *Lyplal1*mice for. The number of WT, Het, and KO mice was studied was, respectively, 28, 31, and 14 for females and 30, 22, and 7 for males. Results are presented as mean ± SEM. *$p < 0.05$ and **$p < 0.01$ between the KO mice and either WT or Het mice. \$$p < 0.05$ between the KO mice and both the WT and Het mice. Statistics were performed on log transformed data. P values were calculated using a students t-test (two-way)

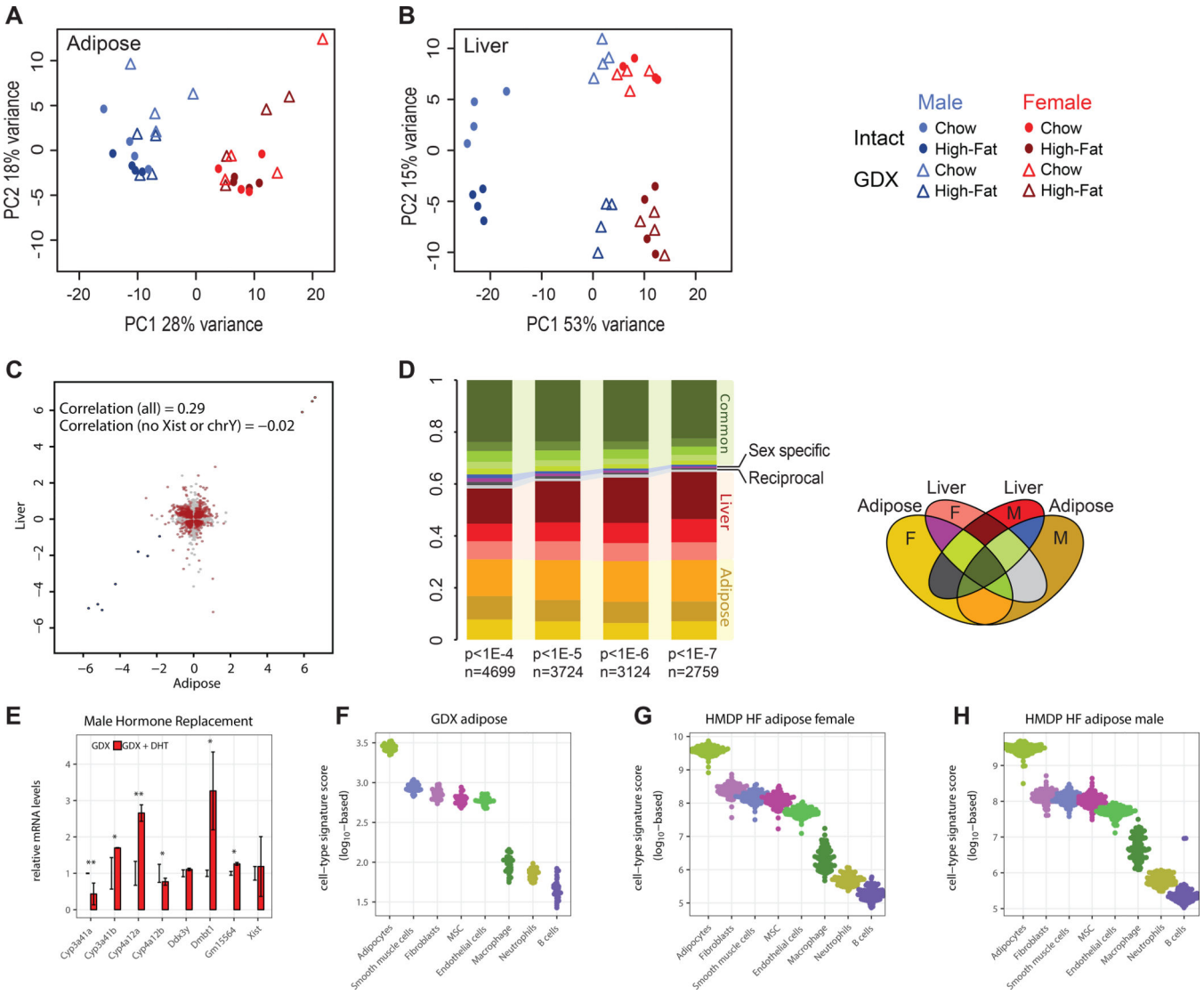

Figure 5. Tissue specificity of Sex differences in regulation of expression.

Total gene expression in adipose (**A**) and liver (**B**) was summarized using principal component analysis (PCA), a data reduction method, in two dimensions for intact mice and gonadectomized mice. Note that the axis in liver and adipose are the same. Dots indicate intact samples, triangles indicate GDX, males are in blue and females are in red, chow diet is in lighter color and high fat diet is darker. In control samples PC1 in both tissues differentiates between sexes, while PC2 corresponds to diet. **C.** Plot of correlation between effects of gonadectomy in liver and adipose. **D.** Sex specificity of expression QTLs (eQTLs) in hfHMDP. eQTLs common to both tissues are in green, adipose specific are in yellow, liver specific are in red, reciprocal are in grey and sex-specific are magenta (females) and blue (males). Color legend on the right indicates the overlapping section of the four datasets **E.** Livers from gonadectomized C57BL/6J male mice with or without testosterone (DHT) pellet administration were analyzed for expression changes corresponding to the top 7 contributing genes to liver principle component variation (shown in Fig S6). Five of the seven genes driving shifts in principle components were shifted back to levels similar to intact mice via

hormone replacement. **F-H.** Adipose deconvolution from gonadectomy experiments, HMDP HF/HS females (**F**), and HMDP HF/HS males (**G**). Results are presented as mean ± SEM. *P<0.05 and **P<0.01 between gonadectomized (GDX) males and gonadectomized males with testosterone implants (DHT). P values were calculated using a students t-test (two-way) n=6 per group and expression normalized to the geometric mean of PPIA and RPL13a.

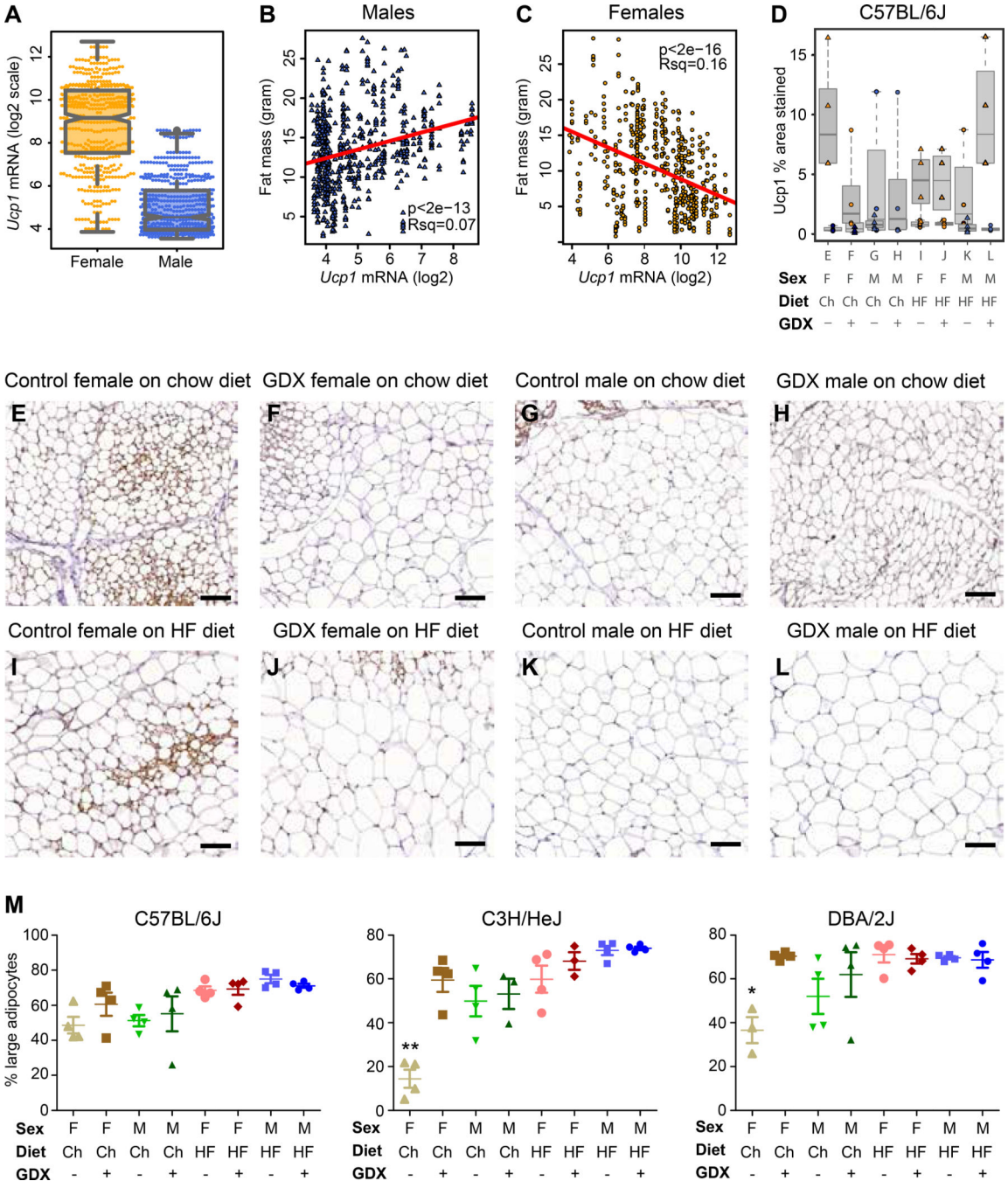

Figure 6. Sex differences in adipose tissue point to mitochondrial function

A. UCP1 expression in female and male adipose tissue in hfHMDP. **B,C.** UCP1 is significantly and inversely correlated to fat mass in males (R=0.26, p<2E-13) and females (R=−0.4, p<2E-16). **D.** Percent area stained for UCP1 in intact and gonadectomized C57BL/6J mice fed chow and HF/HS diets. X axis labels refer to histological panels in **E-L. E-L.** Representative UCP1 staining from gonadal fat of mice. Coding of sex, diet and GDX as in panel **D.M,** Percent of large adipocytes (large/total number of adipocytes) in intact and gonadectomized C57BL/6J, C3H/HeJ and DBA/2J mice mice fed chow or HF/HS diet.

*P<0.05 and **P<0.01 between gonadectomized group (GDX) and sham operated controls. P values were calculated using a students t-test (two-way).

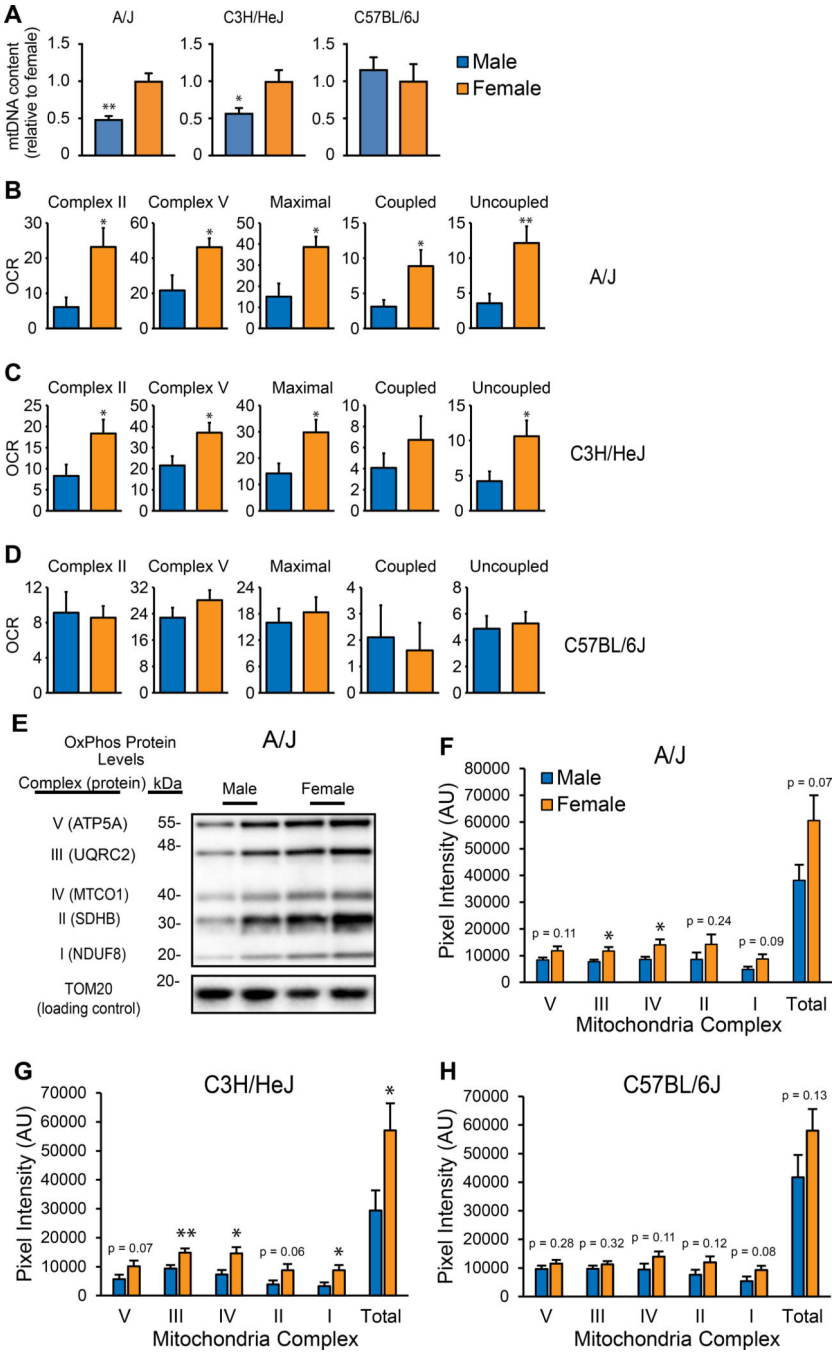

Figure 7. Gene-by-sex interactions in mitochondrial oxidation functions

A. Mitochondrial DNA content were measured in gonadal adipose of A/J, C3H/HeJ and C57BL/6J mice of both sexes. **B-D.** Mitochondria were isolated from gonadal adipose of strains A/J (n = 5 for males and 8 for females), C3H/HeJ (n = 8 for both sexes), and C57BL/6J (n = 8 for both sexes) and oxidative functions tested using a seahorse bioanalyzer. Different mitochondrial states were measured as described in Materials and Methods. Oxygen consumption rate (OCR) was normalized to μg mitochondrial protein (pmol/min/μg protein). Representative immunoblot for A/J (**E**) and corresponding quantification for A/J

(**F**), C3H/HeJ (**G**), C57BL/6J (**H**) of electron transport chain components in adipose mitochondria. Mitochondrial contents were normalized to cellular protein contents for quantification and TOM20 is shown as a loading control. Results are presented as mean ± SEM. *P<0.05 and **P<0.01 between the sexes. P values were calculated using a students t-test (two-way).